FREE-VIBRATION ANALYSIS OF GUYED STRUCTURES

by

Rakesh Saxena

A Thesis
presented to the University of Manitoba
in partial fulfillment of the
requirements for the degree of
Master of Science

Winnipeg, Manitoba

ISBN 0-315-44197-6

FREE-VIBRATION ANALYSIS OF GUYED STRUCTURES

BY

RAKESH SAXENA

A thesis submitted to the Faculty of Graduate Studies of the University of Manitoba in partial fulfillment of the requirements of the degree of

MASTER OF SCIENCE

I hereby declare that I am the sole author of this publication.

I authorize the University of Manitoba to lend this publication to other institutions or individuals for the purpose of scholarly research.

Rakesh Saxena

I further authorize the University of Manitoba to reproduce this publication by photocopying or by other means, in total or in part, at the request of other institutions or individuals for the purpose of scholarly research.

Rakesh Saxena

The University of Manitoba requires the signatures of all persons using or photocopying this publication. Please sign below, and give address and date.

Abstract

A new finite element is formulated for cables which enables a truly three dimensional approach to be adopted for the dynamic analysis of any lattice transmission or communication tower. The generalization, unlike previous proposals, can conveniently accommodate towers with significant geometrical complexities and asymmetry stemming from torque frames and antennae. Furthermore, interactions between the guys and mast of a guyed tower can be investigated readily. The free vibrations of two different towers have been analyzed and the generalization is shown to be accurate and versatile. It also enables the recorded galloping motion of the final, most complex tower example to be examined cursorily from a modal perspective.

Acknowledgements

I wish to express my sincere thanks to Professors N. Popplewell and A. Shah for their continuous guidance and encouragement throughout this work. The invaluable assistance rendered by Mr. P. G. S. Trainor is deeply appreciated. The author gratefully acknowledges the encouragement and timely suggestions of Mr. C. K. Wong, Senior Engineer of Manitoba Hydro and Mr. A. Boyd of Manitoba Telephone System. Finally, the author would like to thank Manitoba HVDC Research Centre, Manitoba Hydro and National Science and Engineering Research Council of Canada for financial support.

CONTENTS

LIST OF FIGURES

LIST OF TABLES

Chapter 1

INTRODUCTION

Electrical transmission and multi-level guyed communication towers form important lifelines in modern society. However these structures can be subjected to severe dynamic loads from unbalanced tensions, galloping of iced cables, impact due to a broken cable, extreme winds, and earthquakes. For example, there have been ice storms followed by prolonged uni-directional winds in the Canadian prairie provinces, and Manitoba in particular, which have produced galloping of guy wires. In 1983, heavy freezing rain combined with moderate wind speeds led to the complete collapse of at least eight transmission and communication towers including a 410-meter (1350-foot) TV-tower. The total loss was estimated to be more than 5 million dollars. Therefore, a realistic assessment of the dynamic characteristics of these structures is required to prevent their damage or failure.

The present study examines methods of obtaining the free vibrations of complex guyed towers with the eventual aim of assessing galloping. The galloping phenomenon involves low 0.1 to 3 Hz frequencies and large (typically 5 to 300 multiples of the conductor's diameter) amplitude, self-excited oscillations of transmission lines in a direction which is transverse to that of a steady, usually 6 to 25 m/s wind [5]. It is caused by asymmetry in a conductor's cross-section due either to ice accretion, which may be as thin as 1 mm or quite short in length for the initiation of vibrations [5], or stranding of the conductor cable itself. Den Hartog [9] has given the classical criterion for aerodynamic instability. However, Cheers [4], Chadha [3], Simpson [21] and Nigol and Buchan [18] have suggested that the additional influence of the twisting of a conductor may be significant too. Although the galloping phenomenon is well documented on iced transmission lines, comparatively little attention has been paid to guyed towers. On the other hand, Novak et al [19] have shown that the galloping of guys can lead to stresses high enough to impair the safety of a guyed tower. Also, in a recent study by Tinkler et al [23], it has been suggested that an ice formation with a distinct longitudinal ridge could cause aerodynamically excited galloping of guys whereas one which has ridges or lumps distributed around part of the circumference and along the length should be stable.

Significant coupling was observed between the guy and tower motions on the most well-documented occasion in Manitoba which led to a serious misalignment of the communication tower's antennae dishes and a loss of signal for an extended period. The vibration was complex, involving multiple-loop oscillation of the guys, concomitant with a damaging flexure of the mast. Therefore, the excited modes were much higher than the fundamental so that a detailed dynamic analysis was undertaken with the aim of determining, ultimately, the types of modes which are most easily excited. However, the existing approximate method of Novak et al [19] ,even with the later refinements of McCaffrey [16] and Tuomo Karna [13], was inadequate. Specifically, these procedures cannot handle practical complexities stemming from offset or non-symmetrically placed antennae dishes. Furthermore, a sloping ground, arbitrary loads and torque frames, which may be used to connect the guys to the tower, invariably present difficulties. Instead, therefore, a somewhat generalized finite element algorithm was developed whose essential new feature is a cable element which can handle 3-dimensional transverse vibrations. Mast segments were modelled as equivalent beams to simplify input data and reduce the size of the global stiffness matrix. An analytical solution for a guyed mast was also formulated by incorporating the dynamic stiffness of a simple wire developed, in a closed form, by Veletsos and Darbre [24] . These theoretical expressions are fairly similar to those developed by Irvine [12] but they can also accommodate guys having large inclinations to the horizontal. The last solution provides a useful check on the finite element method but it is valid only for simple symmetrical towers.

The accuracy and computational efficiency of the present finite element approach, which is termed "generalized" for convenience, will be demonstrated by using two practical towers having progressively more complex geometries. First, a multi-level guyed tower from Wisconsin will be considered. This tower has been analyzed previously by McCaffrey and Hartmann [17] who used a mode summation technique. It is symmetrical so that a further check can be made by utilizing the analytical technique. Then, a multi-level guyed microwave tower, the Manitoba Telephone System (MTS) tower located in the Manitoba province of Canada, will be assessed because it has several offset microwave dishes and torque frames. This tower can be handled only by using the generalized finite element procedure.

Chapter 2

ANALYTICAL METHOD

2.1 Introduction

An analytical method will be developed in the present chapter to study the free vibrations of a guyed tower with a uniform mast. Equations of motion will be derived for the tower's mast and the guys, with both components treated as continuous systems. Thus, modelling should be more accurate than a comparable finite element idealization with reduced degrees of freedom. However, it will be shown that there are computational difficulties associated with the analytical procedure. It is essentially less efficient than a finite element technique. Therefore, only simple towers can be analyzed conveniently. Nevertheless, the usefulness of the analytical technique arises from the fact that the results obtained from approximate methods can be compared and verified for problems of simple geometries like symmetrical towers.

Modelling of the tower, by using the analytical technique, will be described next.

2.2 Modelling the tower

A two-level guyed tower and its equivalent model are shown in Figure-2.1a and b. Consider the case of undamped transverse vibrations. The tower's mast is assumed to be a beam while the guy cables are represented by horizontal frequency-dependent springs each with stiffness K_{gd}. The K_{gd} depends on the circular frequency, ω, of the transverse vibrations. The actual expression for K_{gd} is quite complicated and it is included more conveniently in Section 2.2.2. However, to elucidate the spring's behaviour, consider the horizontal stiffness of the simple oscillator shown in Figure 2.2. It can be seen that the undamped dynamic stiffness is a vector sum of a spring force and an inertial force, both which arise from a unit displacement from the oscillator's static equilibrium position. The frequency dependence of K_d stems from the inertial force.

The dynamic behaviour of a mast and guys will be discussed in the next two sections. The major results derived in these two sections will be incorporated in the third section which examines the guyed tower as a whole.

2.2.1 The mast

A uniform mast, with constant material properties along its length, can be considered reasonably as a beam which, due to its self-weight and guy tensions, is subjected to a compressive axial load. However, it is necessary to subdivide the mast into more than one segment in order to consider the concentrated axial loads arising at each guy level. For example, the 2-level guyed mast shown in Figure 2.1a is divided into three elements. The axial load (due to the self-weight of the mast) varies along the mast's length. However, it is taken to be constant for each element in order to reduce the complexity of the equations of motion. This is a reasonable approximation providing a sufficient number of elements is taken on the mast. Note that the idealization is not the same as that in a finite element formulation because each subdivided mast element still remains a continuous system with an infinite number of degrees-of-freedom.

As the mast is considered to consist of uniform beam elements, consider a uniform beam element acted upon by a compressive load, P (Figure 2.3). The end shear forces, Q_1 and Q_2, and corresponding moments, M_1 and M_2, can be expressed in terms of the end displacements, v_1 and v_2, and rotations, Ω_1 and Ω_2 (Figure 2.4), as follows

$$\begin{Bmatrix} Q_1 \\ M_1 \\ Q_2 \\ M_2 \end{Bmatrix} = \begin{bmatrix} k_{11} & k_{12} & k_{13} & k_{14} \\ & k_{22} & k_{23} & k_{24} \\ \text{symmetric} & & k_{33} & k_{34} \\ & & & k_{44} \end{bmatrix} \begin{Bmatrix} v_1 \\ \Omega_1 \\ v_2 \\ \Omega_2 \end{Bmatrix} \qquad (2.1a)$$

or, in abbreviated form,

$$\{F\} = [K_{bd}]\{U\} \quad . \tag{2.1b}$$

The k_{ij} , $i,j = 1$ to 4, in equation (2.1a) are the elements of a 4x4 elemental dynamic flexural stiffness matrix, K_{bd} . The detailed steps leading from the equation of motion to the precise derivation of K_{bd} are included in Appendix A. It is found that the elements of K_{bd} involve trigonometric and hyperbolic functions of the circular frequency ω. It will be shown later, therefore, that an exact analytical solution is very difficult to obtain. Hence, a numerical procedure will be adopted to compute the natural frequencies. In order to analyze the guyed tower as a whole, the stiffness matrices, K_{bd} are computed for each element of the mast. These elemental matrices are then assembled after including the guy stiffness at each level.

2.2.2 The guy cable

The guys affect the mast's vibrations in two ways. They

1. provide lateral stiffness at the point of attachment to the mast due to the horizontal component of their stiffness; and
2. increase the compressive axial load on the mast due to the vertical components of the tensions.

Figure 2.5 illustrates the forces acting on the mast due to an inclined guy cable attached at point P. The F_{HT} and F_{VT} shown are the horizontal and vertical components of the tension, respectively. In most practical cases, the guys are arranged uniformly at a particular level, about the centre of the mast, so that the algebraic sum of their corresponding F_{HT} values vanishes. The other three forces, i.e., F_V, F_{HI} and F_{HO}, arise due to the horizontal displacement of node P. They can be expressed as

$$F_V = K_V \Delta y \tag{2.2}$$

$$F_{HI} = K_I \Delta x \tag{2.3}$$

$$F_{HO} = K_O \Delta z \tag{2.4}$$

where Δx, Δy and Δz are the displacements of P along the x, y and z directions, respectively. Furthermore, the K_I, K_V and K_O are the dynamic stiffnesses of the guy cable in the corresponding x, y and z directions. The K_I are in the plane of the mast and the guy so that they are called the in-plane horizontal stiffnesses. The K_O, on the other hand, are normal to this plane so that they are termed out-of-plane horizontal stiffnesses. These latter stiffnesses may be derived by considering the case where the upper end, P, of the guy in Figure 2.5 is subjected to a harmonically varying horizontal displacement. The expressions for K_I and K_O are given by Veletsos and Darbre [24] as :

$$K_I = \frac{(1 + 1/2\ \gamma\sigma)^2}{(1 + 12\ \gamma\rho/\phi^2)} (AE/L_e)\cos^2(\theta)$$

$$+ \phi\cot(\phi)\ (T_o/L)\sin^2(\theta) \qquad (2.5)$$

and

$$K_o = \phi\cot(\phi)\ T_o/L \qquad (2.6)$$

where

$$\gamma = 2/\phi\ \tan(\phi/2) - 1 \qquad (2.7)$$

$$\sigma = q_y L/T_o\ \tan(\theta) \qquad (2.8)$$

$$\rho = \frac{1}{12}\ \frac{AE}{T_o}\ \frac{L}{L_e}\ (q_y L/T_o)^2 \qquad (2.9)$$

$$L_e = L\{1 + 1/8\ (q_y L/T_o)^2\} \qquad (2.10)$$

$$\phi = \omega/\omega_o \qquad (2.11)$$

and

$$\omega_o = 1/L\ (T_o/\mu)^{1/2}\ . \qquad (2.12)$$

The description of symbols is as follows.

q_y is the intensity of the normal self load per unit chord length; L is the length of the chord; T_o is the axial component of the guy tension, i.e., the component parallel to the chord; A is the cross-sectional area of the guy; E is the Youngs modulus of elasticity; θ is the inclination of the chord to the horizontal; μ is the mass of the guy per unit of chord length; L_e is the effective guy length; ω is the circular frequency of the actual motion; ω_0 is a reference circular frequency; ϕ is the dimensionless frequency; ρ is the relative stiffness parameter; and σ is a dimensionless parameter which gives a measure of sag.

Various limitations and approximations involved in expressions (2.5) through (2.12) may be summarized as follows.

1. The expressions are valid only for an undamped case.
2. The material is assumed to be linearly elastic so that it obeys Hooke's Law.
3. The guy cable is assumed to be deflected in a parabolic profile at its position of static equilibrium. This latter approximation is reasonable for a cable with a sag-to-span ratio of 1/8 or less [12]. (Another approximation implicit in this assumption is that the component of the load in the direction of the chord due to the weight of the cable has negligible effect on the cable's profile and tension. In practice, this last approximation is justified for small sags because the cable tension is much larger than the weight of the cable.)

4. The displacement amplitude is presumed small so that the cable's motion is considered linear.
5. The inertial forces in the longitudinal direction (along the chord) are negligible in comparison to those in the transverse direction. This approximation is reasonable for cables used as guys because the ratio of the fundamental natural frequency of longitudinal vibrations to that of lateral vibrations is about 40 [12].
6. There is no coupling between the in-plane and out-of-plane motions.

These assumptions and approximations will be discussed further in Chapters 4 and 5 where actual towers will be analyzed.

2.2.3 The guyed tower

Consider next the free vibrations of a complete guyed tower undergoing bending. The analysis for longitudinal and torsional motions will be similar.

When the tower's mast is displaced from its position of static equilibrium, a restoring force tries to bring it back. This restoring force arises from the flexural rigidity of the mast and the lateral dynamic stiffnesses, K_{gd}, of the guys. The K_{gd} is obtained by the vector addition of the in-plane (K_I) and out-of-plane (K_o) horizontal stiffnesses. The latter depend on the arrangement, at any particular level, of the guys about the centre of the mast. For example, if three or more ($n \geq 3$) identical guys are arranged uniformly about the centre of the mast, the expression for K_{gd} will be [24]

$$K_{gd} = n/2 \; (K_I + K_o) \tag{2.13}$$

Here, by assuming linearity, the resistance offered by the guys at any particular level will be proportional to K_{gd}. The K_{gd} is added to the corresponding flexural stiffness term of the stiffness matrix of the mast. Therefore, by using equations (2.1a) and (2.13), the assembled dynamic stiffness matrix for the guyed tower of Figure 2.1a, including the effect of the guys, is given by

$$\begin{Bmatrix} Q_1 \\ M_1 \\ Q_2 \\ M_2 \\ Q_3 \\ M_3 \\ Q_4 \\ M_4 \end{Bmatrix} = \begin{bmatrix} k_{11}1 & k_{12}1 & k_{13}1 & k_{14}1 & & & & \\ & k_{22}1 & k_{23}1 & k_{24}1 & & & & \\ & & \begin{matrix} k_{33}1 \\ +K_{gd_2} \\ k_{11}2 \end{matrix} & \begin{matrix} k_{34}1 \\ + \\ k_{12}2 \end{matrix} & k_{13}2 & k_{14}2 & & \\ & & & \begin{matrix} k_{44}1 \\ + \\ k_{22}2 \end{matrix} & k_{23}2 & k_{24}2 & & \\ & & & & \begin{matrix} k_{33}2 \\ +K_{gd_3} \\ k_{11}3 \end{matrix} & \begin{matrix} k_{34}2 \\ + \\ k_{12}3 \end{matrix} & k_{13}3 & k_{14}3 \\ & & \text{symmetric} & & & \begin{matrix} k_{44}2 \\ + \\ k_{22}3 \end{matrix} & k_{23}3 & k_{24}3 \\ & & & & & & k_{33}3 & k_{34}3 \\ & & & & & & & k_{44}3 \end{bmatrix} \begin{Bmatrix} v_1 \\ \Omega_1 \\ v_2 \\ \Omega_2 \\ v_3 \\ \Omega_3 \\ v_4 \\ \Omega_4 \end{Bmatrix} \tag{2.14}$$

Here the superscripts on k_{ij}s denote the element number idealizing the tower mast.

Now the external force vector vanishes for free vibrations. Also, the tower's base is fixed so that $v_4 = \Omega_4 = 0$. Therefore equation (2.14) simplifies to

$$\begin{bmatrix} k_{11}^1 & k_{12}^1 & k_{13}^1 & k_{14}^1 & & \\ & k_{22}^1 & k_{23}^1 & k_{24}^1 & & \\ & & k_{33}^1 + K_{gd2} + k_{11}^2 & k_{34}^1 + k_{12}^2 & k_{13}^2 & k_{14}^2 \\ & & & k_{44}^1 + k_{22}^2 & k_{23}^2 & k_{24}^2 \\ & \text{symmetric} & & & k_{33}^2 + K_{gd3} + k_{11}^3 & k_{34}^2 + k_{12}^3 \\ & & & & & k_{44}^2 + k_{22}^3 \end{bmatrix} \begin{Bmatrix} v_1 \\ \Omega_1 \\ v_2 \\ \Omega_2 \\ v_3 \\ \Omega_3 \end{Bmatrix} = \{0\} \qquad (2.15a)$$

or, alternatively,

$$[K_d]\{U\} = 0 \; . \qquad (2.15b)$$

As seen already (equations(2.5) through (2.12) and Appendix A), both the guys' stiffnesses as well as the mast's stiffness contain terms which are trigonometric and hyperbolic functions of the natural frequency. Therefore, equation (2.15b) is, by definition, a set of homogeneous transcendental equations. For a non-trivial solution

$$\det\,[\,K_d\,] = 0 \; . \qquad (2.16)$$

The roots, ω, i=1, 2, - - - - ∞, of the last equation must be obtained numerically because a general method of solution exists only in the case of polynomial-form equation with the degree of polynomial less than five. Hence, a computer program was developed by using an Incremental Search Method, to compute the natural frequencies and the corresponding mode shapes.

2.3 Discussion of numerical efficiency

A detailed numerical study of the analytical method discussed in this chapter revealed the following advantages.

1. By using the Incremental Search Method, the natural frequencies and corresponding mode shapes can be computed within any frequency range. This is particularly useful to check for the natural frequencies of the tower which lie in a given frequency band of an external forcing function like that of a wind.
2. The dynamic stiffness matrix, K_d, is symmetric and most of the off-diagonal elements are zero as indicated in Figure 2.6. Hence, a semi-bandwidth storage mode can be adopted which requires only 4n elements to be stored for a nxn matrix. The 4n should be compared to n^2 in a full storage mode and $n(n+1)/2$ in a half storage mode. In a practical case when $n \gg 1$, $4n \ll \{ n(n+1)/2 \text{ or } n^2 \}$ so that a significant saving can be achieved in computer storage by using semi-bandwidth storage mode.

3. Savings in storage lead to the possibility of analyzing a multi-level guyed tower with relatively less difficulty than in the case of an approximate method. For example, in the case of a five-level guyed tower with three guys at each level, the size of the stiffness matrix in the analytical method will be 12x12. On the other hand, by using the finite element formulation with ten elements taken on the mast with four degrees-of-freedom assigned to each node and 12 elements on each guy with three degrees-of-freedom to each guy node, the size of the stiffness matrix will be 531x531.

However, the analytical method has the following shortcomings.

1. The solution procedure for computing the natural frequencies may not reveal all the natural frequencies. This problem is best illustrated by considering the plot of K_d as a function of circular frequency, ω, shown in Figure 2.7 . The actual root and the discontinuity lie very close together because the curve becomes almost vertical at the point of discontinuity. Hence, there is a high possibility of missing a root.
2. The dynamic stiffnesses of all the guys, at a particular level, are first lumped and then added to the dynamic flexural stiffness matrix of the mast. There-

fore, the separate mode shapes of the guys at a particular level cannot be computed easily.

3. It is not feasible to develop partial differential equations of motion which can take into consideration arbitrarily spaced guys, cross-arms, torque frames. Hence, the analytical method is applicable to only towers which have a simple geometry.

Chapter 3

NUMERICAL METHODS

3.1 Introduction

This chapter reviews several numerical techniques which avoid the difficulty of a frequency dependent stiffness matrix. However, many of these numerical techniques suffer from some over simplification in the modelling of the mast or guys. The chapter concludes with a description of a generalized 3-dimensional finite element technique which was developed in this thesis. The generalized method incorporates a new finite element for the cable and it is demonstrated to be an accurate and convenient method for the free vibration analysis of a guyed tower.

Several numerical methods for the dynamic analysis of the guyed tower have been employed in the past. In 1966, Hartmann and Davenport [10] suggested a mode summation technique in which the displacements of the mast and guys were represented by a summation of generalized time coordinates multiplied by assumed mode shapes. The equations of motion for the guy were derived by using a Newtonian method whilst the mast equations were developed using by Lagrange's technique. The resulting two sets of coupled equations were written in a matrix form in which the generalized time coordinates for the guys and the mast formed the vector of unknowns. The equations could be solved for the free vibration case to obtain the natural frequencies and corresponding mode shapes for the guy-mast system. A limitation in this study was that only the lowest frequency in-plane mode of each guy was considered. However, it has been observed that the lowest natural frequency of a guy of a tall mast is typically in the range of 0.2 to 0.6 Hz while the galloping vibrations generally occur in the range of 0.2 to 3 Hz [13]. Hence, many vibration modes of the guys may be needed to account for the interaction between the mast and the guys. Also, usually more than five guy modes are needed to investigate the galloping phenomenon [13]. However, Davenport's [6] model may suffice in case of gusty wind whose spectrum is confined to the low frequency region. In 1972, McCaffrey and Hartmann [17] presented a paper on the dynamics of guyed towers. Their method was similar to that developed by Hartmann and Davenport [10] but was more general as it could also include non-symmetricity in mass and stiffness matrices. The method was applied to a five-level guyed tower. Further, a more accurate catenary guy model was compared with the much simpler parabolic approximation and it was observed that these two guy models predicted natural frequencies which differed by as much as 4% . Also, as most of the lower frequencies were due to guys it was found to be necessary to consider guy modes higher than the fundamental. The mast's mode shapes were assumed to be those of a freely vibrating uniform cantilever of constant flexural rigidity (EI).

Essentially, these mode shapes are over simplified since concentrated forces occur at the guy attachment points and the mast may be non-uniform. Hence, an exact deflection curve cannot be achieved even in an infinite summation.

In a mode summation technique, the number of mast and guy modes which needs to be considered generally depends upon the rate of convergence while computing the natural frequencies and the mode shapes. In addition, higher guy modes might be important from the point of view of guy-mast interaction or galloping of cables.

In 1981, Wright [25] reported on several simple tower dynamic analysis methods in which the guy was considered as a massless taut wire. Thus, the inertial force due to the guy was neglected which predicted the tower frequencies those were higher than the exact values. Nevertheless, these simpler methods give results which might be useful in preliminary design analysis. In 1984, Tuomo Karna [13] proposed a method where the mast was described by simplified lumped masses and the undamped in-plane mode shapes of the guys were used as Ritz shape functions. The resulting equations were solved in the frequency domain.

In the present work a generalized 3-dimensional technique is proposed. The next section describes the modelling of the different components constituting the guyed towers.

3.2 Modelling

The universal features of the distinct components of mast, guys, cross-arms and torque frames which may comprise different transmission and communication towers will be outlined next. Assumptions used to formulate their dynamic properties by using the finite element procedure will be summarized first. Then, further simplifications to justify the mode summation or analytical procedures will be highlighted. Relative difficulties arising from the necessarily different numerical solutions of the resulting equations of motion will be indicated.

3.2.1 The Mast

A mast can be reasonably considered to consist of beam elements, each having a uniform weight distribution [22]. An individual beam will be assumed to possess the now standard three rotational and three translational degrees-of-freedom at each end. The resulting conventional 12x12 consistent mass and stiffness matrices can be found in reference [20]. However, the former matrix will be diagonalized in the most complex tower example by lumping masses equally at the ends to alleviate the then excessive computations. The moment of inertia I, needed to compute the flexural rigidity EI, of a lattice mast segment corresponds reasonably to the inertia of its cross-section [22]. Illustrative procedures for triangular cross-sections are presented in Appendix B. However, the basic stiffness matrix does not include the compressive loads due to a cable's tension, the weight of higher elevation elements and the self-weight of the element itself. Such loads can be incorporated straightforwardly into the basic stiffness matrix by employing the standard geometric stiffness matrix described, for example, in reference [15] . This procedure was followed selectively in generating new results.

3.2.2 Guy Cables

The new cable element has the typical geometry shown in Figure 3.1b where a node has the three degrees-of-freedom u, v and w. Now u and v are the displacements in the longitudinal and transverse directions which are, respectively, along and perpendicular to the chord, whilst w is the displacement out of the plane of sag. Thus, this cable element can represent a three dimensional motion. Details of the final element stiffness matrix are given more conveniently in Appendix B. The formulation was verified by correlating results with the known free vibrations of a single inclined cable and it will be shown in Section 3.2.2.1 that 8 to 16 elements provide a reasonable representation of a single cable. It should be noted that the same assumptions made for the guy analysis in the analytical approach also apply here. However, the effect of the longitudinal inertia can be investigated in the present modelling by including the corresponding terms in the mass matrix. The finite element results for the cable will be compared with theoretical solutions outlined in the next section.

3.2.2.1 Theoretical studies

There have been several studies [6,7,8,12,14,24] which have developed an expression for the dynamic stiffness of an inclined cable subjected to a prescribed harmonic displacement at the upper end while the bottom end is fixed. In 1947, Kolousek [14] gave a series solution for a uniform, undamped cable deflected in a parabolic profile at its position of static equilibrium. Davenport [6] in 1959 published a paper which condensed Kolousek's series solution to a closed form. In 1961, Dean [8] gave an expression for the dynamic guy modulus by using a catenary profile. However, he neglected the elastic stretch of the cable. Later in 1965, Davenport and Steels [7] generalized Kolousek's series solution to include the effect of a uniform external damping. McCaffrey and Hartmann [17] in 1970 presented approximate series solution for an undamped cable whose static deflection was a catenary. In 1978, Irvine [12] gave a solution for undamped parabolic cable which was essentially identical to that of Davenport. Recently, in 1983, Veletsos and Darbre [24] presented a closed-form solution for damped cables.

Figures 3.2a to c show the in-plane horizontal dynamic stiffness, K_I , as a function of the circular frequency, ω, for an undamped inclined guy cable. The three different models of Davenport [6], Irvine [12], and Veletsos [24] are given. It can be seen that all the curves correspond at ω = 0 to the static case with a positive dynamic stiffness. This indicates that the cable force opposes the mast's displacement. However, with increasing frequency, the stiffness decreases to zero and ultimately becomes negative. The negative stiffness indicates that the cable force, instead of providing support to the mast, acts in phase with the mast's motion. The stiffness asymptotically approaches minus infinity which is a point of discontinuity. It restarts at plus infinity and follows the same trend with further increases in frequency. A zero dynamic stiffness corresponds to a natural frequency of the guy cable whose ends are fixed-free. An infinite stiffness, conversely, corresponds to a natural frequency for the case of fixed-fixed ends. In the latter case there are two modes of vibration which are symmetric and antisymmetric. In the case of an antisymmetric mode, no overall additional tension is induced in the cable at its ends. A symmetric mode, on the other hand, generates an overall additional tension. It should be noted, however, that an antisymmetric distribution of additional tension is possible so that the overall additional tension is zero. Irvine [12] has compared the peak additional tensions on the basis of identical amplitudes of vibration in both the antisymmetric and symmetric in-plane modes. On comparing the first antisymmetric and first symmetric modes for a cable of deep profile, the ratio of additional tensions is found to be about 20% .

Comparing the three models of dynamic stiffness , it can be noted that both Irvine and Davenport have not included the antisymmetric mode. Figure 3.2d shows a plot of the out-of-plane dynamic stiffness K_o as a function of ω. In this case the natural frequencies for the fixed-fixed case are same as those of a taut cable.

Figures 3.3a to d show plots of the in-plane dynamic stiffness obtained from the finite element approach. As the number of elements is increased from six to sixteen, the natural frequencies approach those predicted by Veletsos. Using a 16-element model, the maximum discrepancy in the first six natural frequencies is found to be less than 4% .

3.2.3 Cross-Arms and Torque Frames

Guys are often attached to a mast by triangular cross-arms called torque frames in order to increase the tower's torsional stiffness. A typical torque frame is shown in Figure 3.4a where it can be seen that a frame normally consists of non-symmetrical, short lattice members. The shear deformations of these frames cannot be ignored because they are not "slender" [22]. Hence, unlike the mast, the frame cannot be modelled as a series of beams. Nevertheless, its mass and stiffness matrices can be derived by considering plausible motions at the extremities. The extremity consisting of the four (normally close) attachment points to the mast can be assumed to remain planar in accordance with the small vibration constraint of the overall linear theory. Consequently, the left vertical plane in Figure 3.4b will undergo the three translations and three rotations illustrated. The torque frame's right extremity is essentially a point to which the guys are attached so that three translations should suffice. Thus, a torque frame's motion can be normally described largely by nine components at the two extremities. The resulting 9x9 static stiffness matrix can be computed by separately applying unit forces and moments, commensurate with the nine degrees of freedom, and noting the ensuing movements. This procedure was performed by using the readily available computer package SAPIV [2] for static analyses. The corresponding mass matrix was formed by lumping and proportioning the total mass of the frame according to the translational degrees-of-freedom.

3.2.4 Microwave Dish

A microwave dish is normally a short, stiff conical section which protrudes from the mast of a communication tower. It is treated, therefore, in Appendix B as a deadweight which is off-set from a finite element node of the mast by means of a rigid horizontal member. Both the off-set's translation and rotation may profoundly affect a dish's alignment which must remain within $1/2^0$ of the original orientation to preserve communications.

3.2.5 Complete Tower

The element mass and stiffness matrices developed previously can be selected appropriately for the form of a particular tower. They can be combined conventionally [1] to give the equations of motion in the eigenvalue form

$$\left[[K] - \omega^2 [M]\right] \{V\} = \{0\} \tag{3.1}$$

for a freely vibrating tower. Matrices [K] and [M] correspond to the assembled global stiffness and mass matrices, respectively; eigenvalue ω is the circular natural frequency and $\{V\}$ is the corresponding eigenvector describing the relative motions of a given mode. Eigenvalues and eigenvectors were computed by using either the subspace iteration procedure [1] or the standard IMSL package [11] depending which was more advantageous from the viewpoint of storage requirement and computational time. The subspace iteration incorporated a skyline technique [1] of storing the matrix system in order to alleviate potential storage difficulties arising from the usually large order, n, of the sparsely populated [K] and [M].

3.3 Comparison with other approaches

Rather than presume deflection fields within small finite elements, McCaffrey [16] assumed that the whole mast and each complete guy moved in a series of modes. Then the so called "mode summation technique" parallels somewhat the finite element procedure but the final eigenvalue problem's order can be reduced by around 95% ! The technique's accuracy, however, depends critically upon the preciseness of the assumed modes. Mode shapes can be estimated reasonably *a priori* when, as in the situation considered by McCaffrey, the mast is fairly uniform without complicating appendages or asymmetries, guys vibrate predominantly in one plane and the lowest frequency (or most easily imagined) modes dominate. Such conditions, however, rarely arise in practice.

In contrast, the analytical procedure is essentially a hybrid implementation of the generalized finite element and the mode summation strategies. A mast is treated as a series of equivalent beams, which are continuous and uniform between consecutive guy attachments, whereas each guy is considered as a whole. It can be seen that the final dynamic stiffness matrix, $[\ K_d(\omega)\ ]$, does not have the separate mass and stiffness form of equation (3.1). Indeed, $[\ K_d(\omega)\ ]$ contains transcendental functions of the circular frequency, ω, which make the necessarily numerical solution more tedious. A straightforward incremental search was adopted to calculate the zeros of the determinant of the dynamic stiffness matrix, Det[$K_d(\omega)$], and, hence, the natural frequencies. However, there is no sophisticated means of determining all the zeros with certainty so that increasingly finer increments of ω (which, of course, involve proportionately more computations) may be needed.

Chapter 4

WTMJ TOWER

4.1 Introduction

In the present chapter, the free vibrations of a symmetrical multi-level guyed tower will be studied by using the generalized finite element technique. Comparisons will be made with the analytical model and an earlier study by McCaffrey [16].

4.2 The tower

The WTMJ Tower is a five-level, guyed television tower located in Milwaukee, Wisconsin, U.S.A. In planform it has three equally spaced guys at each level which are connected directly to the mast as illustrated in Figure 4.1a. The mast consists of piecewise prismatic sections whose properties are listed in reference [16]. SAPIV does not have provision to include the cable elements so that comparisons will be made with the analytical model and an earlier study by McCaffrey and Hartmann [17]. The tower was modelled by using 16 cable elements for each guy whilst the mast was idealized by 47 prismatic beam elements. This idealization leads to 282 nodes and 957 degrees-of-freedom.

The first two columns in Table 4.1 give the natural frequencies of the lowest modes obtained by using the analytical model and the generalized finite element approach. The maximum discrepancy is a respectable 5% . The first, third and eleventh modes involve significant coupling between the mast (in bending) and the guys. Then the tower's uppermost 30 metres, corresponding to the antenna, dominates the mast's bending because its flexural rigidity is only about 0.1% of that of the lower sections. The omission of all but the first and last natural frequencies in the next two columns of Table 4.1, which correspond to the additional neglect of all the guys' out-of-plane stiffnesses, suggests that the majority of the previous modes involve predominantly out-of-plane guy motions. Thus, only the two retained modes have guys which move in-plane and interact noticeably with the mast.

The last column in Table 4.1 relates to the model of McCaffrey [16]. McCaffrey neglected the guys' out-of-plane stiffnesses again so that, not surprisingly, he reasonably predicted only the first and the last frequencies in column 1 and 2 of Table 4.1. (However Table 4.2 suggests that even higher natural frequencies where guys display purely in-plane movements are still estimated fairly well.) He also assumed that the mast's mode shapes corresponded to those of a freely vibrating, uniform cantilever beam having a constant flexural rigidity. The validity of this assumption can be assessed by reference to Figures 4.1b and c where the various predictions of the mast's movement alone, relative to its tip, are presented for the first and eleventh modes. Analytical and finite element results agree, of course, but they produce a less smooth change in slope than the mode summation procedure near the top of the mast. Thus, the uniform beam assumption does not completely account for the sudden transition expected between the mast and antenna due to their significantly different flexural stiffnesses.

In summary, the generalized finite element technique gives comparable results to the analytical and, if mode shapes are anticipated reasonably and fully, the mode summation procedure. However, only the former technique can be applied readily to problems which, as in the next example, involve a variety of structural components generating a commensurately complex tower geometry.

Chapter 5

MTS TOWER

5.1 Introduction

In the present chapter, a multi-level guyed tower, the MTS tower, will be assessed in which the complex geometry necessitates the use of the generalized finite element approach.

5.2 The tower

The MTS tower illustrated in Figure 5.1a is a lattice microwave tower having four circular antenna dishes positioned at the elevations shown in Figure 5.1b. Like the WTMJ tower, it has five guy levels which are located symmetrically in planform. However, although the third level has three guys connected directly to the mast as in the WTMJ tower, each of the other four levels has six guys joined to a torque frame. A torque frame is offset from the mast to give the mast extra torsional stiffness. It is incorporated in the generalized finite element procedure by creating a member with nine degrees-of-freedom in the manner described in Section 3.2.3. Microwave dishes, on the other hand, are treated as large masses which are offset rigidly from finite element nodes of the mast. Details of the procedure to calculate the dishes' moments of inertia are presented in Appendix B. Also, given in Appendix B for completeness is the way of determining the moment of inertia of a beam element which is equivalent to that of the lattice mast's triangular cross-section.

Computational effort is beneficially reduced in any finite element analysis by minimizing the total number of elements used and the bandwidth of the final dynamic stiffness matrix [1] . Such requirements become more acute as sizes increase but they have to be mitigated by the opposing demand of more elements for usually improved accuracy. Then, for a given element idealization, the bandwidth can be minimized by a skillful numbering of the nodal points. Of particular interest here is an adequate but concise representation of the guy wires which may exhibit damaging interactions with the mast in the 0.1 to 3 Hz galloping prone range. Preliminary calculations which approximated the inclined guys by using pinned-pinned ends suggested a representation of 16, 16, 10, 8 and 8 cable elements for the top through lowest guys, respectively. Thus, there should be a reasonably accurate three nodes minimum per half-loop of guy movement below 3 Hz. At least seventeen beam elements was needed to represent the mast's geometric and material changes and to easily accommodate microwave dishes and guy connections. This resulted in 1014 total degrees-of-freedom and the optimum nodal numbering gave a bandwidth of 191.

It was found that the lowest 100 or so natural frequencies of the MTS tower involved primarily guy motions. Consequently, the IMSL eigenvalue package was used only in this particular example to avoid simultaneously finding these somewhat superfluous modes in addition to the desired modes having more guy-mast coupling. The present behaviour contrasts with that of the WTMJ tower where three out of the first eleven modes exhibited significant guy-mast coupling. The contrast arises because the MTS tower has almost twice the number of guys with tensions which are 3 to 10 times lower than those for the WTMJ tower. Consequently, the guy stiffnesses of the WTMJ tower are more nearly comparable to the stiffness of its mast which leads to greater coupling at the lowest frequencies.

Table 5.1 lists those natural frequencies below 3 Hz in which noticeable coupling occurs between the MTS mast and its guys. The effects on such natural frequencies of an axial load (from the tensions in the guys and the mast's own weight), temperature and icing may be determined from this table. Indeed, the first two columns indicate that the axial load has only a marginal reducing effect on a typical day of 20°C. The three central columns, on the other hand, show that temperature reductions from 20°C through 0°C to -12°C consistently raise the frequencies quite noticeably and also introduce progressively more guy-mast couplings. The increase occurs because a temperature decrease produces higher tensions in the guys whose combined (stiffening) effect more than compensates the opposing influence of the resulting compressive load on the mast. Problems with freezing rain can arise when air temperatures are at or somewhat below $0^{o}C$ so that the rain freezes on contact with a guy to form a more galloping susceptible, asymmetrical cross-section. For simplicity, however, the 3/8" radial thickness icing associated with the fifth column of Table 5.1 is assumed to be distributed symmetrically around and along the entire length of each guy. The difference should be anticipated to be significant only when, unlike in the present theory, an off-axis centre of mass is permitted to twist a guy about its own geometric axis [21]. The third and fifth columns of Table 5.1 show that the heavy icing alone reduces the natural frequencies associated with conspicuous (flexurally vibrating) guy and mast interactions by up to an appreciable 12% . A similar reduction happens too for the omitted, dominantly guy modes and it is caused, not surprisingly, by the additional mass of the ice. Distributed ice accretions with smaller masses, therefore, should produce almost correspondingly lower percentage frequency changes. Table 5.1 also suggests that a heavy ice deposit significantly increases the number of interactive modes which may make the tower more vulnerable to galloping.

Figure 5.2(a) presents an idea of the MTS tower's motion obtained from a video recording on the day following a freezing rain storm and after a loss of communication had been detected. Later enquiries at the nearest Meteorological Office indicated that, on the day of the recording, the affected region had a temperature around -12°C and a steady wind of about 8 m/s blowing from the north-west to the south-east. Thus, Figures 5.1(c) and 5.2(a) suggests that merely the virtually windward guys were galloping appreciably but only at the second and fourth levels. The icing on the galloping guys occurred intermittently and was probably very light because it was difficult to discern clearly. These guys, therefore, are likely quite close to an ice-free condition. Indeed, two ice-free modes whose natural frequencies almost coincide with vibrations actually observed at 0.83 Hz in the fourth level windward guy and at 1.67 Hz in the second level windward guy and the mast are also given in Figures 5.2(b) and (c), respectively. As expected, the first such theoretical mode involves only the fourth level guys whereas the latter has coupling between the mast and the second level guys. Although a combination of these modes seems to be predominantly excited in the galloping situation, it is the coupled one which presumably leads to the misalignment of the mast-attached microwave dishes. The major outstanding question, however, is : why did the downwind second and fourth level guys (whose theoretical modal motions, according to Figures 5.2(b) and (c) relate strongly to the corresponding upwind guys) barely oscillate in the field ? The answer remains uncertain but may be related to local aerodynamic damping fluctuations caused by small changes in the guys' effective orientations to the wind [9]. Obviously, this point bears further investigation.

Chapter 6

CONCLUSIONS

An analytical technique has been extended and applied here to a symmetrical tower having no off-set components. Results agree reasonably with those derived from a mode summation approach and a generalized finite element procedure. However, the generalized finite element procedure has been shown to be particularly useful for a guyed tower possessing often used off-set dishes and torque frames. It is also able to straightforwardly accommodate even more complicated asymmetrical geometries. The effects of typical axial loads on a mast, temperature and icing of the guys have been investigated. Severe icing produces the largest shifts in the natural frequencies and greater coupling between the mast and guys of a guyed tower. Limited field data suggests that a coupled mode of the guyed MTS tower could well have led to misalignment of its microwave dishes after a freezing rain storm.

REFERENCES

1. Bathe, K. J.,"Finite Element Procedures in Engineering Analysis", Prentice-Hall, Inc., NJ-07632, 1982.
2. Bathe, K. J., Wilson, E. L. and Peterson, F. E., "SAPIV - A Structural Analysis Program for Static and Dynamic Response of Linear Systems", Report EERC 73-11, College of Engineering, Univ. of Calif., Berkley, June 1973, revised April 1974.
3. Chadha, J., "Ontario Hydro Research Division Report", No. 73-399-K, 1973.
4. Cheers, F., "A Note on Galloping Conductors", NRC Canada, Lab. Technical Report MT-14, 1950.
5. Currie, I. G., Harvard, D. G. and Pon, C. J., " Literature Survey on Aeolian Vibration Excitation of Bundled Conductors", Canadian Electrical Association (CEA) Spring Meeting, Vancouver, 1987.
6. Davenport, A. G., "The Wind-induced Vibrations of Guyed and Self-supporting Cylindrical Columns", Trans. Eng. Inst. Can. 3, pp. 119-141, 1959.
7. Davenport, A. G. and Steels, G. N., "Dynamic Behaviour of Massive Guy Cables", J. Struct. Div., ASCE 91, no. ST2, pp. 43-70, 1965.
8. Dean, D. L., " Static and Dynamic Analysis of Guy Cables", J. Struct. Div., ASCE 87, no. ST1, pp. 1-21, 1961.

9. Den Hartog, J. P., "Transmission Line Vibrations due to Sleet", Trans. AIEE, vol. 51, pt 4, pp. 1074-1086, 1932.

10. Hartmann, A. J. and Davenport, A. G., "Comparison of the Predicted and Measured Dynamic Response of Structures to Wind (Sante Fe Railroad Floodlight Tower)", University of Western Ontario, Faculty of Engineering Science Research Report, ST-1-66, 1966.

11. International Mathematical and Statistical Libraries (IMSL), Inc., Houston, Texas, 1984.

12. Irvine, H. M., "Cable Structures", MIT Press, 1981.

13. Karna, T., "Dynamic and Aeroelastic Action of Guy Cables", D.Tech. Thesis, Lab. of Struct. Engng., Finland, 1984.

14. Kolousek, V., "Solution Statique et Dynamique des py lones d'antenne haubanes", Publ. Int. Assoc. Bridge Struct. Eng. 8, pp. 105-140, 1947.

15. Mathur, R. K., "Structural Dynamic Characteristics of the Transmission Systems", M.Sc. Thesis, Dept. of Civil Engng., Univ. of Manitoba, Winnipeg R3T 2N2, 1985.

16. McCaffrey, R. J., "Dynamics of Guyed Towers", M.Sc. Thesis, Marquette University, Milwaukee, Wisconsin, Aug. 1969.

17. McCaffrey, R. J. and Hartmann, A. J., "Dynamics of Guyed Towers", J. Struct. Div. ASCE 98, pp. 1309-1323, 1970.

18. Nigol, O. and Buchan, P. G., "Conductor Galloping - Part I and II", IEEE Transactions on Power Apparatus and Systems, Vol. PAS-96, No. 2, pp. 699-720, Feb. 1981.

19. Novak, M., Davenport, A. G. and Tanaka, H., , "Vibrations of Towers due to Galloping of Iced Cables", Jour. of Engng. Mech. Div., Proc. of ASCE, Vol. 104, No. EM2, pp. 457-473, Apr. 1978.

20. Przemieniecki, J. S., "Theory of Matrix Structural Analysis", McGraw-Hill, 1968.

21. Simpson, A., "Wind-Induced Vibration of Overhead Power Transmission Lines", Sci. Prog., 68, pp. 285-308, 1983.

22. Timoshenko, S., "Theory of Elastic Stability", McGraw-Hill, New York, 1960.

23. Tinkler, J., Popplewell, N. P. and Shah, A., "Effects of Freezing Rain on Guyed Towers", Int. Conf. on Flow Induced Vibrations, Bowness-on-Windermere, England, May 1987.

24. Veletsos, A. S. and Darbre, G. R., "Dynamic Stiffness of Parabolic Cables", Earthquake Engng. and Structural Dynamics, Vol. 11, pp. 367-401, 1983.

25. Wright, A. D.,"Tower Dynamics Analytical Models : Comparison and Evaluation", Rocky Flats Wind Systems Program, Dec. 1981.

Appendix A

THE ANALYTICAL MODEL FOR THE MAST

An analytical model for a mast in transverse bending will be developed in the present section. The mast is considered to consist of uniform beam elements and one such uniform beam element of length λ, acted upon by a compressive load, P, is shown in Figure 2.3. The equation of motion can be written in terms of the transverse displacement, $V(x,t)$, where x is the spatial coordinate along the element's axis and t is time. Consequently,

$$d^2/dx^2 \, (E'I' \, d^2V/dx^2) + \rho' \, d^2V/dt^2 + d/dx \, (P \, dV/dx) = 0 \qquad (A.1)$$

where E'I' is the flexural rigidity and ρ' is the mass per unit length. Equation (A.1) can be solved by employing the Separation of Variables and assuming

$$V(x,t) = v(x) \sin(\omega t). \qquad (A.2)$$

The $v(x)$ in equation (A.2), which depends only on x, is called the shape function. The ω is the circular frequency of the beam element's free vibration in transverse motion. Substituting $V(x,t)$ from equation (A.2) into equation (A.1) and solving for $v(x)$, leads to

$$v(x) = C_1 \cos(b_1 x) + C_2 \sin(b_1 x)$$

$$+ C_3 \cosh(b_2 x) + C_4 \sinh(b_2 x). \qquad (A.3)$$

The C_i, $i = 1$ to 4, are four constants which have to be evaluated by considering the four boundary conditions, two at each end of the beam element. Also,

$$b_1 = \{(\alpha^4 + \beta^4/4)^{1/2} + \beta^2\}^{1/2} \qquad (A.4)$$

$$b_2 = \{(\alpha^4 + \beta^4/4)^{1/2} - \beta^2\}^{1/2} \qquad (A.5)$$

where

$$\alpha^4 = \rho' \omega^2 / E'I' \qquad (A.6)$$

and $\beta^4 = P/E'I'$. (A.7)

It can be seen from equation (A.3) that the shape function, v(x), involves trigonometric and hyperbolic functions of the circular frequency ω . It will be shown later, therefore, that an exact analytical solution is very difficult to obtain. Hence, a numerical procedure will be adopted to compute the natural frequencies.

Figures A.1(a) and (b) give the sign conventions for the shear force and bending moment which can be expressed in terms of shape functions as :

$$V(x) = -E'I'v(x)''' - Pv' \qquad (A.8)$$

$$M(x) = E'I'v(x)'' \qquad (A.9)$$

From Figures A.1(a) and (b),

$$\begin{aligned}
Q_1 &= -V_0 = E'I'v_0''' + Pv_0' \\
M_1 &= -M_0 = -E'I'v_0'' \\
Q_2 &= -V_\lambda = -E'I'v''' + Pv' \\
M_2 &= M_\lambda = E'I'v'' \,.
\end{aligned} \qquad (A.10)$$

From equations A.3 and A.10,

$$\begin{Bmatrix} Q_1 \\ M_1 \\ Q_2 \\ M_2 \end{Bmatrix} = \begin{bmatrix} 0 & -E'I'b_1{}^3+Pb_1 & 0 & E'I'b_2{}^3+Pb_2 \\ E'I'b_1{}^2 & 0 & -E'I'b_2{}^2 & 0 \\ -E'I's_1b_1{}^3+Psb_1 & E'I'c_1b_1{}^3-Pc_1b_1 & -E'I's_2b_2{}^3-Ps_2b_2 & -E'I'c_1b_2{}^3-Pc_1b_2 \\ -E'I'c_1b_1{}^2 & -E'I's_1b_1{}^2 & E'I'c_1b_2{}^2 & E'I's_2b_2{}^2 \end{bmatrix} \begin{Bmatrix} C_1 \\ C_2 \\ C_3 \\ C_4 \end{Bmatrix} \qquad (A.11)$$

where $c_1 = \cos b_1\lambda$, $s_1 = \sin b_1\lambda$,

$c_2 = \cosh b_2\lambda$ and $s_2 = \sinh b_2\lambda$. (A.12)

Equation A.11 can be written in abbreviated form as :

$$\{F\} = [Z]\{\eta\} \,. \qquad (A.13)$$

From equations A.3 and A.12,

$$\begin{Bmatrix} v_1 \\ \Omega_1 \\ v_2 \\ \Omega_2 \end{Bmatrix} = \begin{Bmatrix} v(0) \\ v'(0) \\ v(\lambda) \\ v'(\lambda) \end{Bmatrix} = \begin{bmatrix} 1 & 0 & 1 & 0 \\ 0 & b_1 & 0 & b_2 \\ c_1 & s_1 & c_2 & s_2 \\ -s_1 b_1 & c_1 b_1 & s_2 b_2 & c_2 b_2 \end{bmatrix} \begin{Bmatrix} C_1 \\ C_2 \\ C_3 \\ C_4 \end{Bmatrix} \tag{A.14}$$

or,

$$\{U\} = [W]\{\eta\} \ . \tag{A.15}$$

From equations (A.13) and (A.15), the end shear forces, Q_1 and Q_2, and corresponding moments, M_1 and M_2, can be expressed in terms of the end displacements, v_1 and v_2, and rotations, Ω_1 and Ω_2, as follows

$$\begin{Bmatrix} Q_1 \\ M_1 \\ Q_2 \\ M_2 \end{Bmatrix} = \begin{bmatrix} k_{11} & k_{12} & k_{13} & k_{14} \\ & k_{22} & k_{23} & k_{24} \\ \text{Symmetric} & & k_{33} & k_{34} \\ & & & k_{44} \end{bmatrix} \begin{Bmatrix} v_1 \\ \Omega_1 \\ v_2 \\ \Omega_2 \end{Bmatrix} \tag{A.16}$$

or, in abbreviated form,

$$\{F\} = [K_{bd}]\{U\} \ . \tag{A.17}$$

where $[K_{bd}] = [Z]\ [W]^{-1}$. (A.18)

The elements of the symmetric dynamic stiffness matrix $[K_{bd}(\omega)]$ are given as:

$$k_{11} = k_{33} = b_1 b_2 (b_1{}^2 + b_2{}^2)(b_1 c_2 s_1 + b_2 c_1 s_2)$$

$$k_{12} = -k_{34} = b_1 b_2 (b_2{}^2 - b_1{}^2)(c_1 c_2 - 1) + 2 b_1{}^2 b_2{}^2 s_1 s_2$$

$$k_{13} = -b_1 b_2 (b_1{}^2 + b_2{}^2)(b_1 s_1 + b_2 s_2)$$

(A.19)

$$k_{14} = -k_{23} = b_1 b_2 (b_1{}^2 + b_2{}^2)(c_2 - c_1)$$

$$k_{22} = k_{44} = (b_1{}^2 + b_2{}^2)(b_2 c_2 s_1 - b_1 c_1 s_2)$$

$$k_{24} = (b_1{}^2 + b_2{}^2)(b_1 s_2 - b_2 s_1)$$

where $K_{bd}(\omega) = (E'I'/\Delta)\ k_{ij}$, $i,j = 1,4$

and (A.20)

$$\Delta = \{2 b_1 b_2 (1 - c_1 c_2) - s_1 s_2 (b_1{}^2 - b_2{}^2)\} .$$

Appendix B

Properties of Individual Tower Elements

Formulae needed to compute the elemental stiffness contributions of a guy cable, latticed mast or a microwave dish will be given here for completeness.

(a) Mast with lattice cross-section

Latticed masts usually have a horizontal cross-section which is either square or triangular. Both WTMJ and MTS masts possess a constant triangular form. The following formulae were used to calculate the principal moments of inertia for the MTS masts' flexural stiffnesses. For the case of the WTMJ tower these values were obtained from reference [16].

(i) Triangular cross-section

By using the dimensions indicated in Figure B.1,

$$I_{xx} = 0.5\, I_{yy} = I_{zz} = (A'/4)(2\, c^2 + 3\, r^2) \qquad (B.1)$$

where

$$A' = \pi\, r^2 \qquad (B.2)$$

is the cross-sectional area of each (circular) main leg with radius r.

(ii) Microwave dish

The plan and side view of a typical microwave dish (mounted on a triangular latticed mast) is presented in Figures B.2(a) and (b), respectively. The principal moments of inertia for the axes shown are

$$I_{xx} = I_{yy} = \frac{M'}{4} (R^2 + 4 d^2) \tag{B.3}$$

and

$$I_{zz} = M' R^2/2 \quad . \tag{B.4}$$

where M' and R are the mass and radius of the dish, respectively. The d is the mean distance, in planview, of the dish from the vertical y axis.

(b) Cable Element

The characteristic movement of a guy cable and an illustration of the partial nomenclature describing the dynamic deflection of its typical element are given in Figures 3.1(a) and (b), respectively. At the instant shown, point P_1 and P_2 are located at (x_1,v_1) and (x_2,v_2) with respect to the global co-ordinates x and y. The shortest span between the ends of the complete cable is L but the cable is deformed due to the pretension force, T_0, and its self-weight per unit span normal to the chord, q_y. A guy cable is usually uniform with a constant cross-sectional area, A, mass per unit length, ρ'', and modulus of elasticity E'. Thus, following the lead of Veletsos and Darbre [24], the cable is presumed to have no flexural rigidity. Furthermore, the component of the cable's self-weight along the chord is considered not to affect the cable's parabolic static equilibrium profile or the tension. Finally, the linear theory of vibrations is assumed. This is justified for typically observed sag-to-span ratios less than 1/8 [12].

By using the above assumptions, it was shown in reference [15] that the stiffness matrix of a cable element, having a total six degrees-of-freedom, can be written in the form

$$\begin{bmatrix} k_{xx} & k_{xy} & 0 & -k_{xx} & -k_{xy} & 0 \\ & k_{xy} & 0 & -k_{xy} & -k_{yy} & 0 \\ & & k_{zz} & 0 & 0 & -k_{zz} \\ & \text{symmetric} & & k_{xy} & -k_{yy} & 0 \\ & & & & k_{yy} & 0 \\ & & & & & k_{zz} \end{bmatrix} \quad . \qquad (B.5)$$

Components in the above matrix are given by

$$k_{xx} = \left(\frac{1}{1+\rho_m}\right) \frac{A\ E'}{L'_e}$$

$$k_{yy} = \left\{\frac{1}{2} \frac{q_y}{T_0} (L - x_2 - x_1)\right\}^2 \left(\frac{1}{1+\rho_m}\right) \left(\frac{A\ E'}{L'_e}\right) + \left(\frac{T_0}{x_2-x_1}\right)$$

$$k_{xy} = \left(\frac{1}{1+\rho_m}\right)\left(\frac{A\ E'}{L'_e}\right)\left\{\frac{1}{2}\ \frac{q_y}{T_0}\ (\ L - x_2 - x_1\ )\right\} \tag{B.6}$$

$$k_{zz} = \frac{T_0}{x_2 - x_1}$$

where

$$L'_e = \int_{x_1}^{x_2} [\ 1 + \frac{1}{2}\ \{\ \frac{q_y}{2\ T_0}\ (\ L - 2\ x\ )\}^2]^3\ dx$$

$$\rho''' = \frac{1}{12}\ \left(\frac{A\ E'}{T_0}\right)\left(\frac{L}{L'_e}\right)\left(\frac{q_y\,L}{T_0}\right)^2 \tag{B.7}$$

and

$$\rho_m = \rho'''\left(\frac{x_2 - x_1}{L}\right)^3 \quad .$$

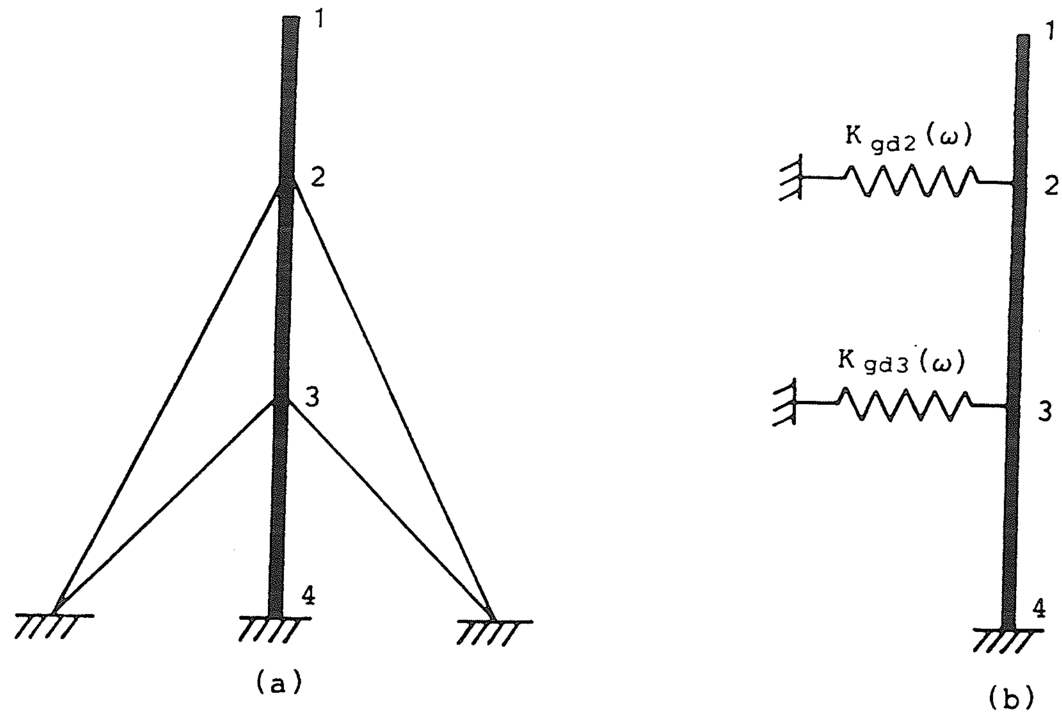

Figure 2.1 (a) A two-level guyed tower and (b) its equivalent model.

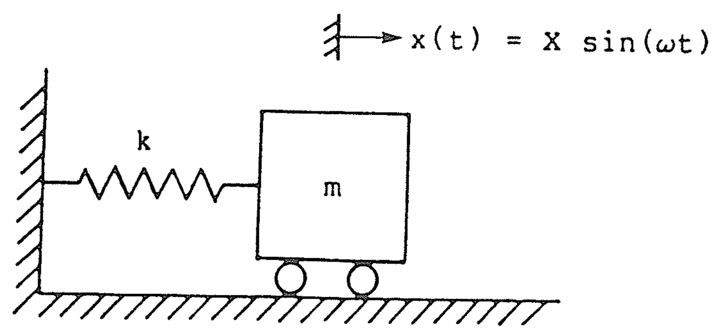

Figure 2.2 A single-degree-of-freedom oscillator whose undamped dynamic stiffness is $K_d(\omega) = k - \omega^2 m$.

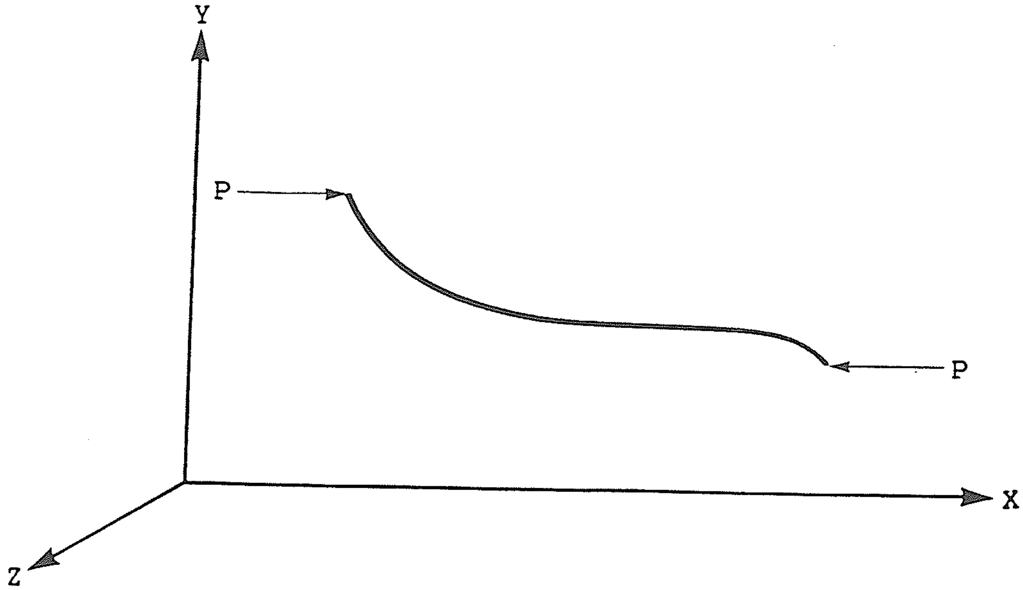

Figure 2.3 A uniform beam element subjected to an axial load, P.

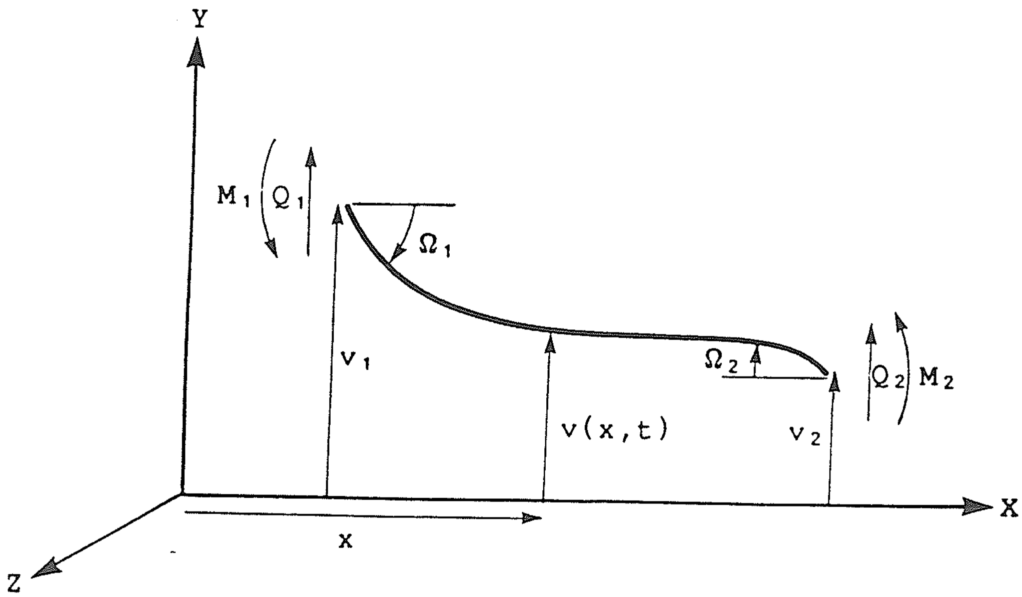

Figure 2.4 The convention used for beam forces (Q_1, Q_2), moments (M_1, M_2), displacements (v_1, v_2) and rotations (Ω_1, Ω_2).

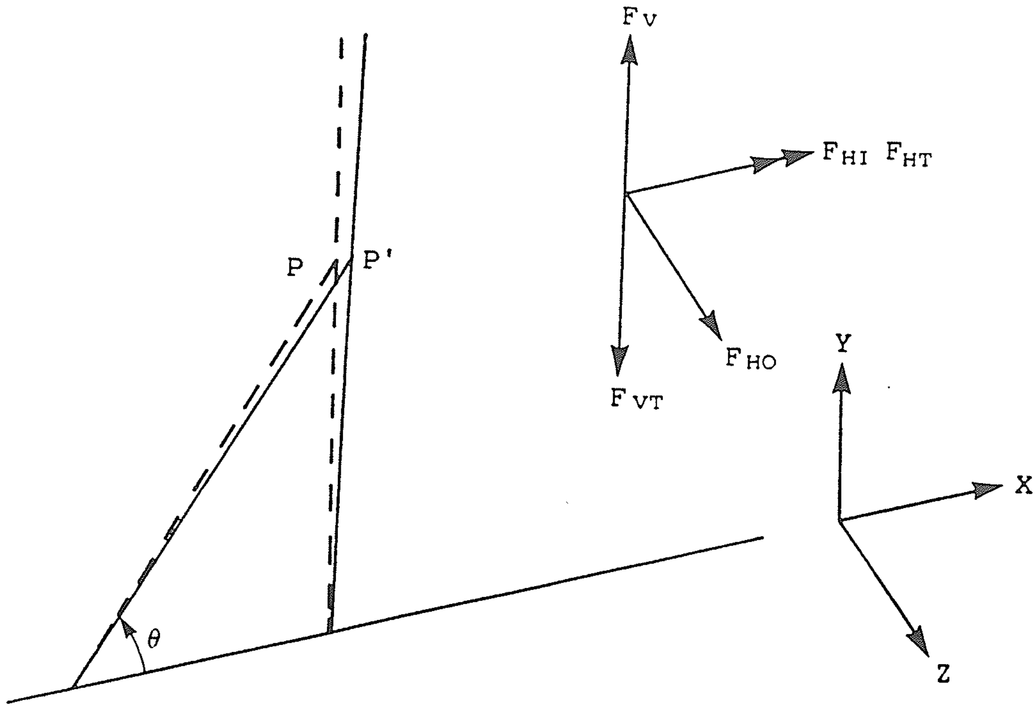

Figure 2.5 The forces at mast node, P', when P' is displaced from its original position, P.

$$\left[\begin{array}{cccccccccc}
X & X & X & X & & & & & & \\
 & X & X & X & & & 0 & & & \\
 & & X & X & X & X & & & & \\
 & & & X & X & X & & & & \\
 & & & & X & X & X & X & & \\
 & & & & & X & X & X & & \\
 \multicolumn{5}{c}{\text{symmetric}} & & X & X & X & X \\
 & & & & & & & X & X & X \\
 & & & & & & & & X & X \\
 & & & & & & & & & X
\end{array}\right]$$

Storage mode	Number of elements stored
Full	n^2
Upper triangle	$n(n+1)/2$
Semi-bandwidth	$4n$

Figure 2.6 The form of the nxn dynamic stiffness matrix K_d.

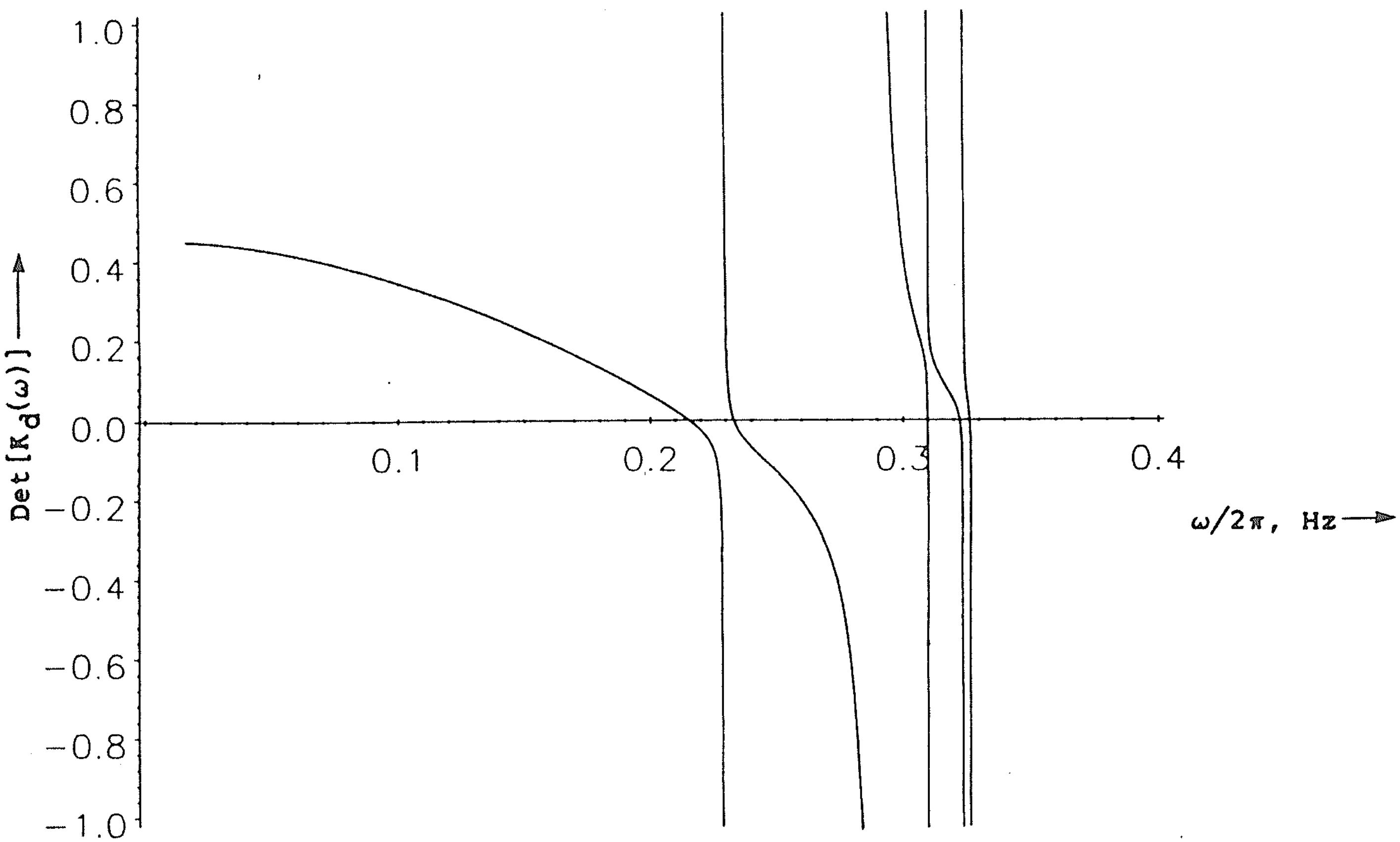

Figure 2.7 Variation with frequency of the determinant of the dynamic stiffness matrix.

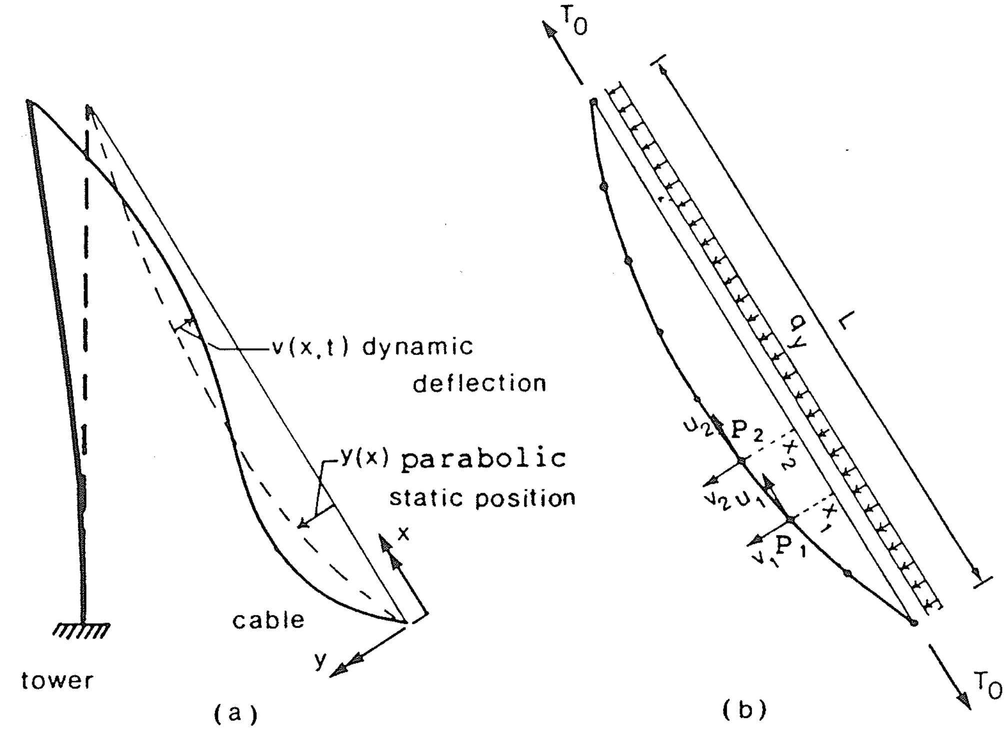

Figure 3.1 In-plane configuration of an inclined cable.

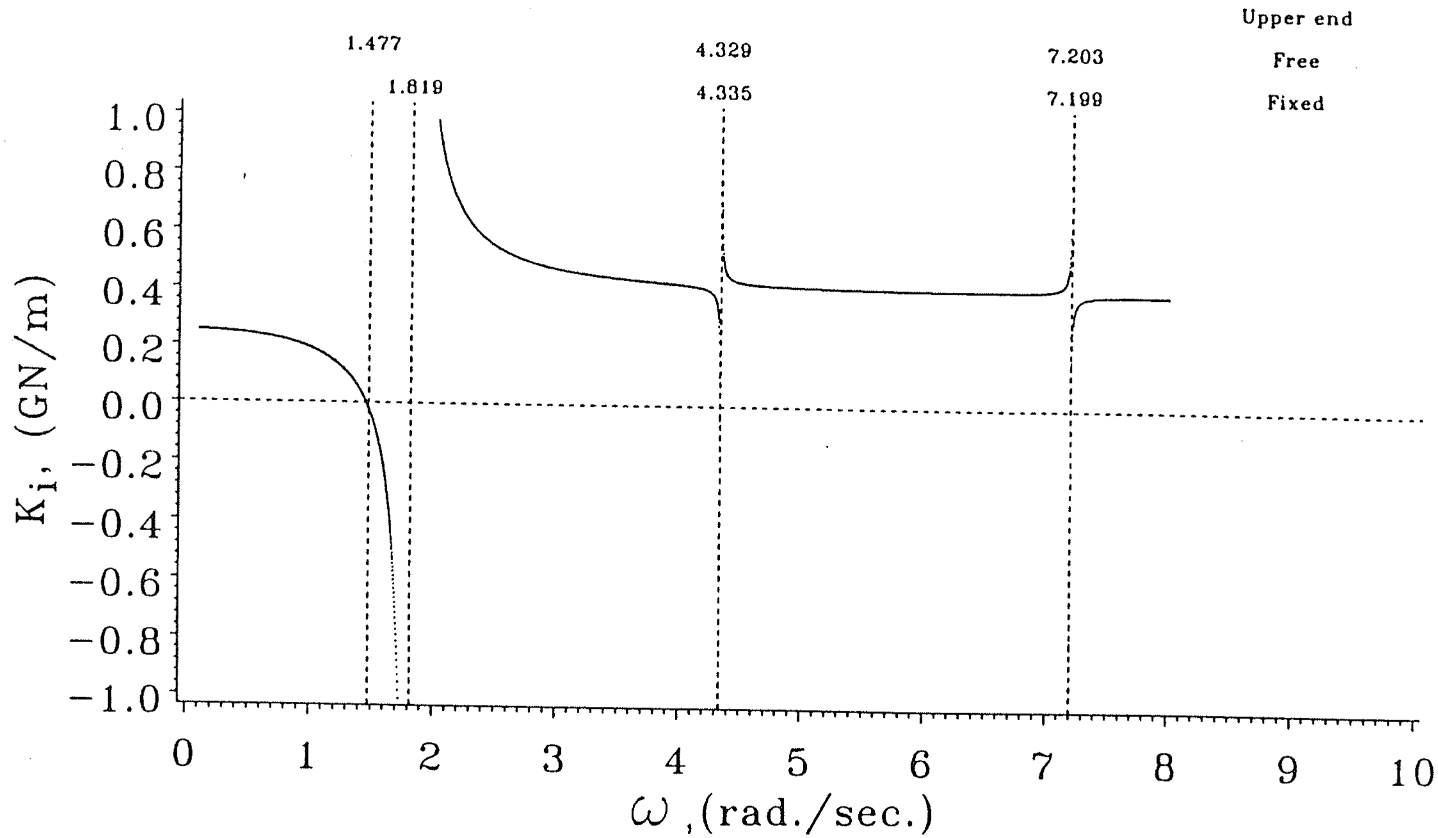

Figure 3.2(a) Variation of in-plane dynamic stiffness with frequency for an undamped inclined cable using Davenport's model. This example corresponds to the 5th level guy of the WTMJ tower.

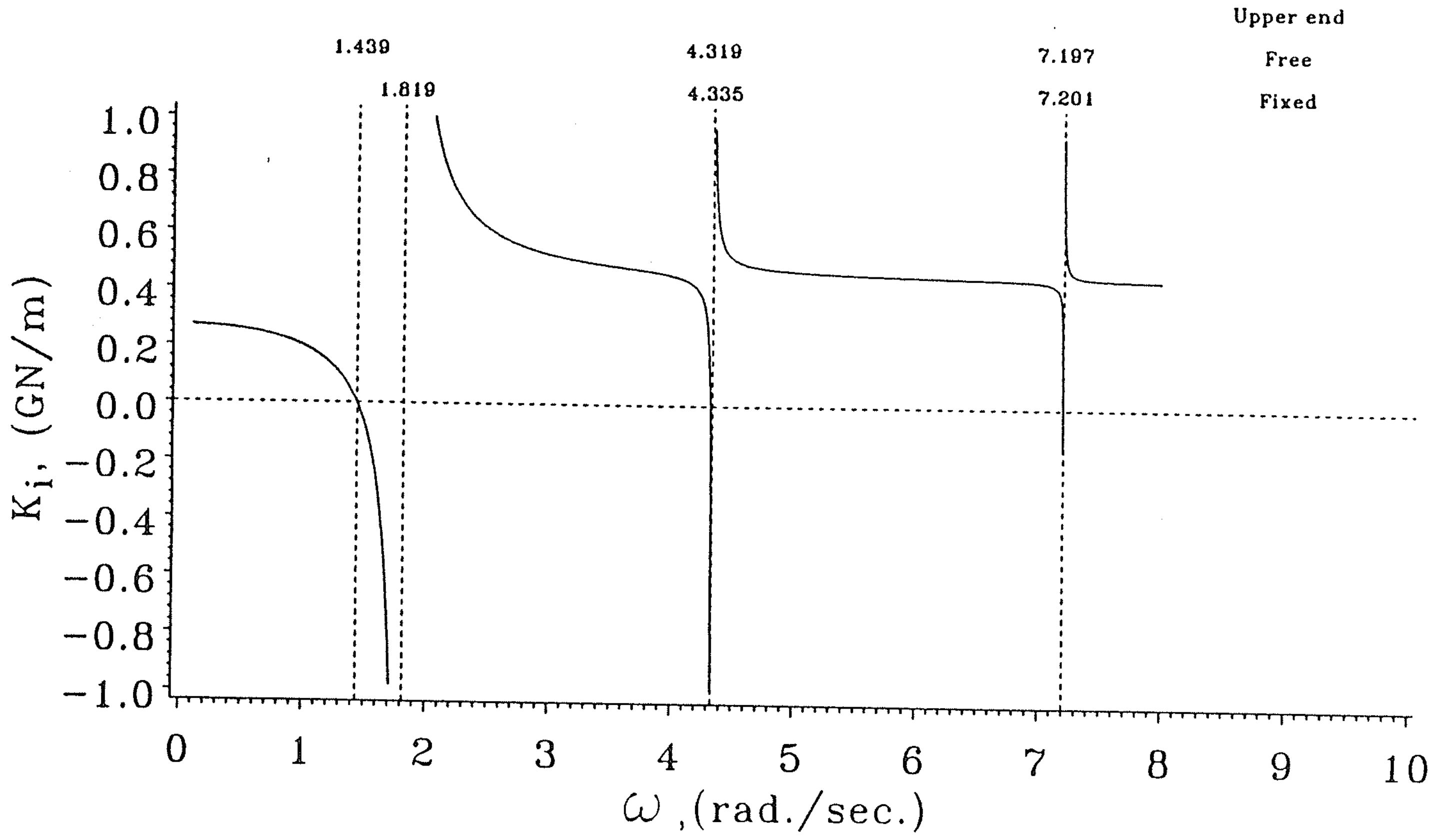

Figure 3.2(b) Variation of in-plane dynamic stiffness with frequency for an undamped inclined cable using Irvine's model. This example corresponds to the 5th level guy of the WTMJ tower.

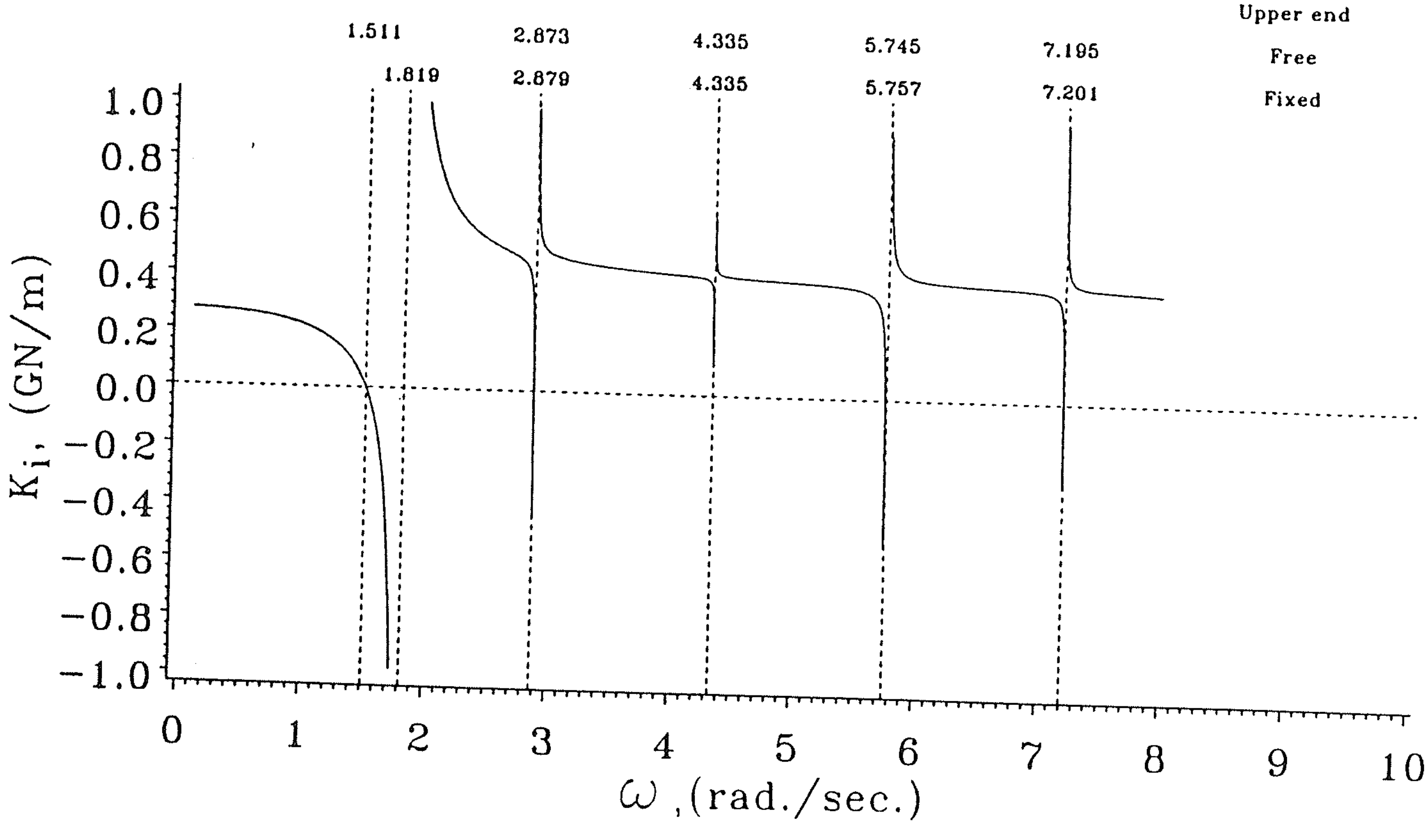

Figure 3.2(c) Variation of in-plane dynamic stiffness with frequency for an undamped inclined cable using Veletsos's model. This example corresponds to the 5th level guy of the WTMJ tower.

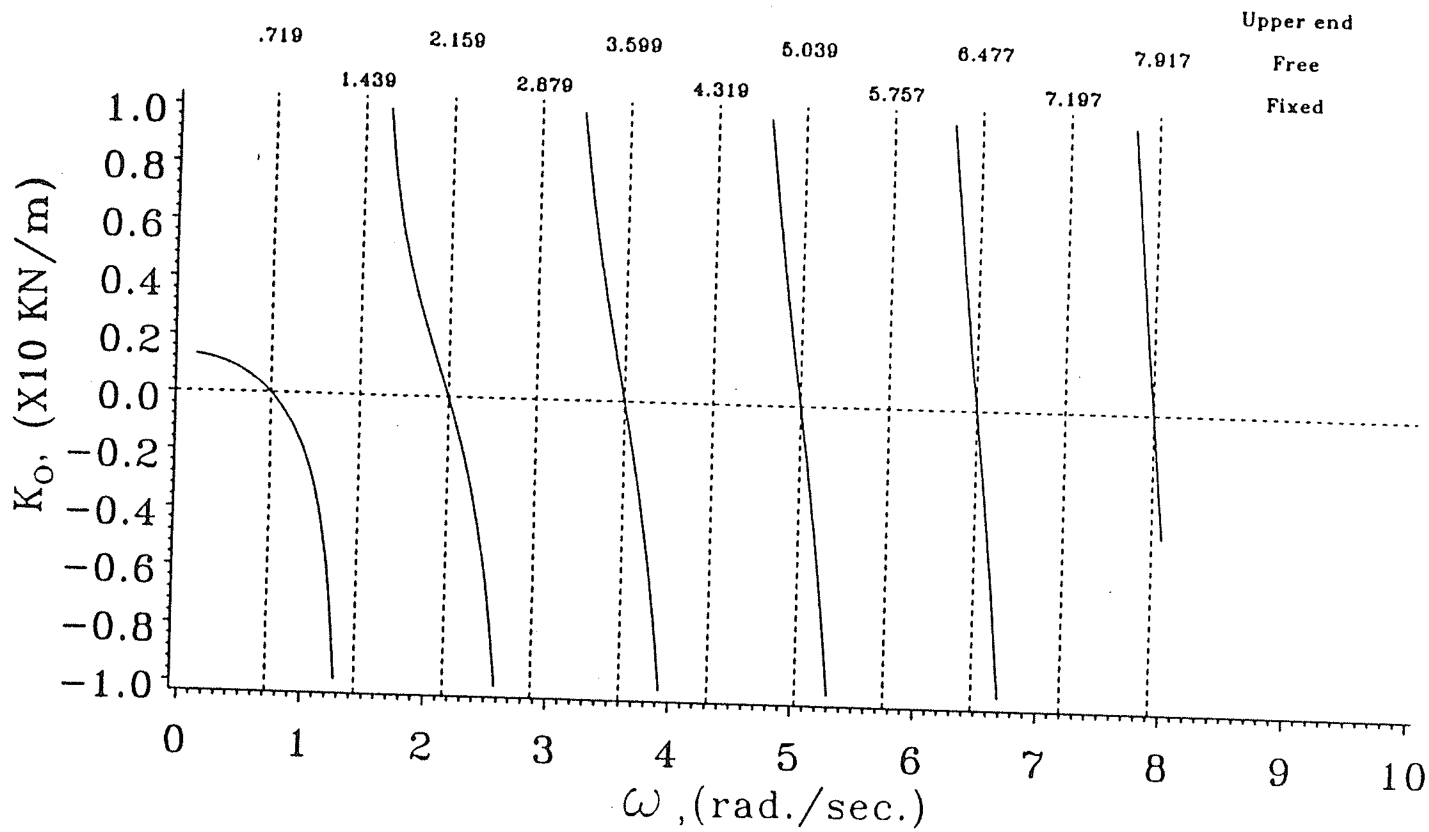

Figure 3.2(d) Variation of out-of-plane dynamic stiffness with frequency for an undamped inclined cable using Veletsos's model. This example corresponds to the 5th level guy of the WTMJ tower.

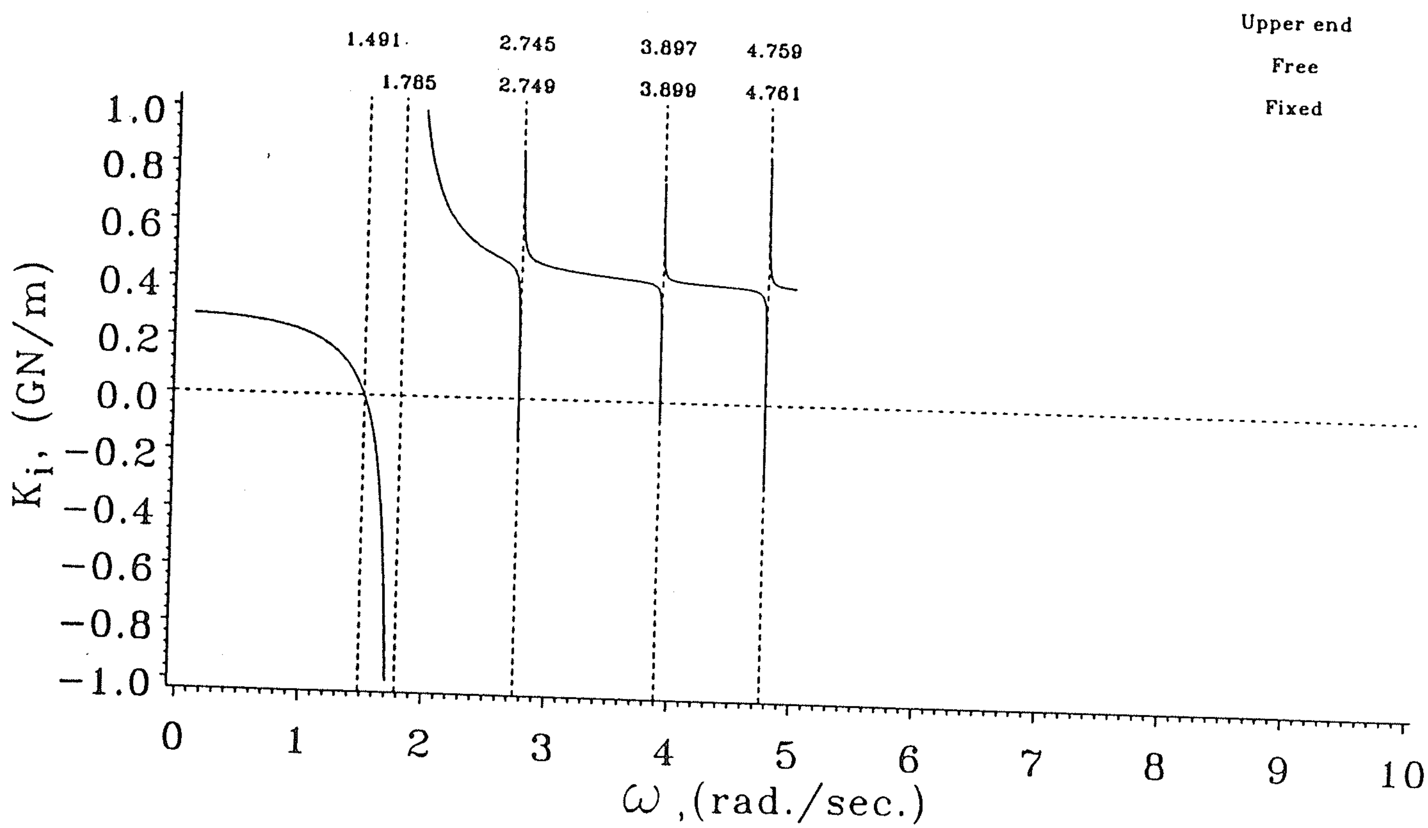

Figure 3.3(a) Variation of in-plane dynamic stiffness with frequency for an undamped inclined cable using FEM model with 6 elements. This example corresponds to the 5th level guy of the WTMJ tower.

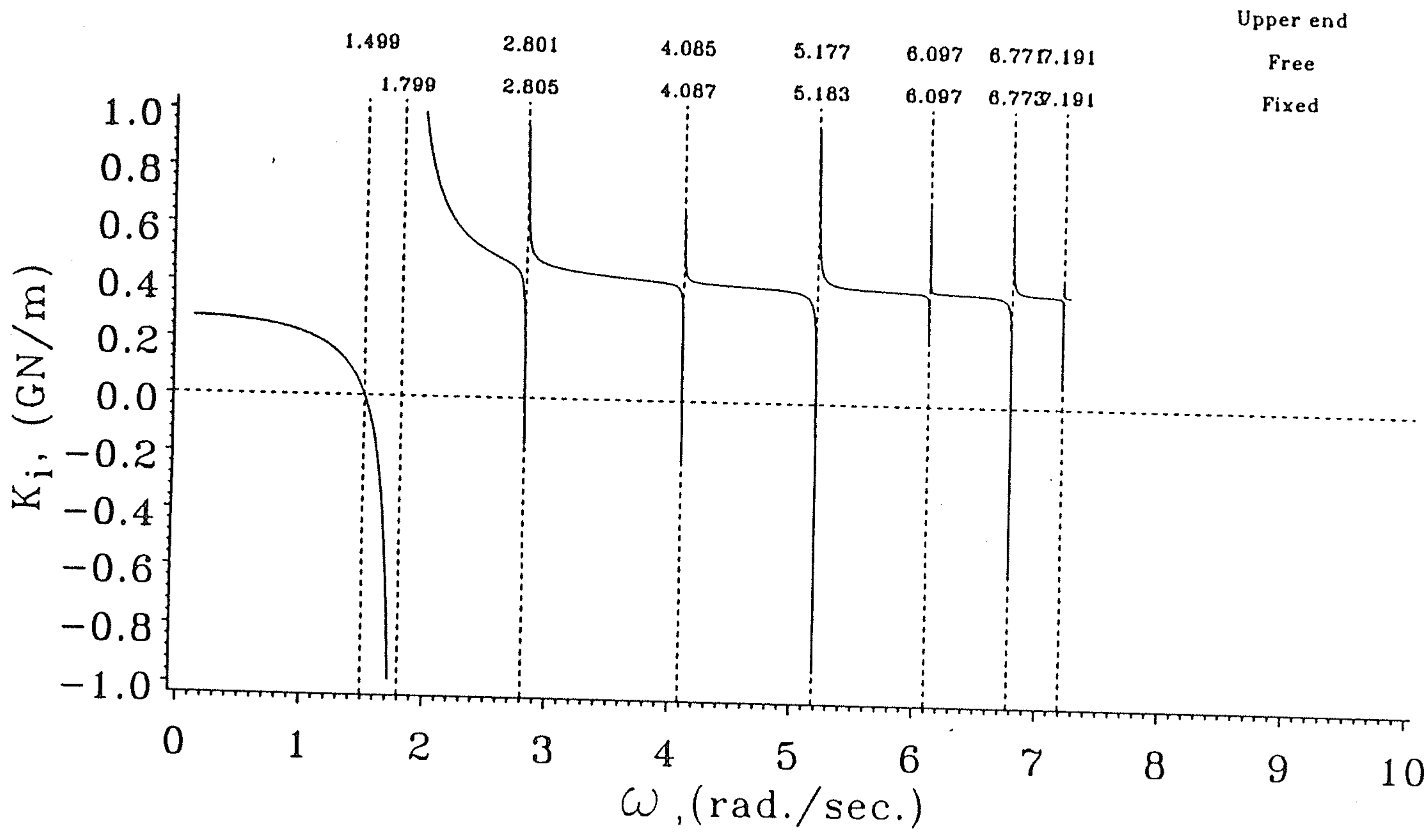

Figure 3.3(b) Variation of in-plane dynamic stiffness with frequency for an undamped inclined cable using FEM model with 8 elements. This example corresponds to the 5th level guy of the WTMJ tower.

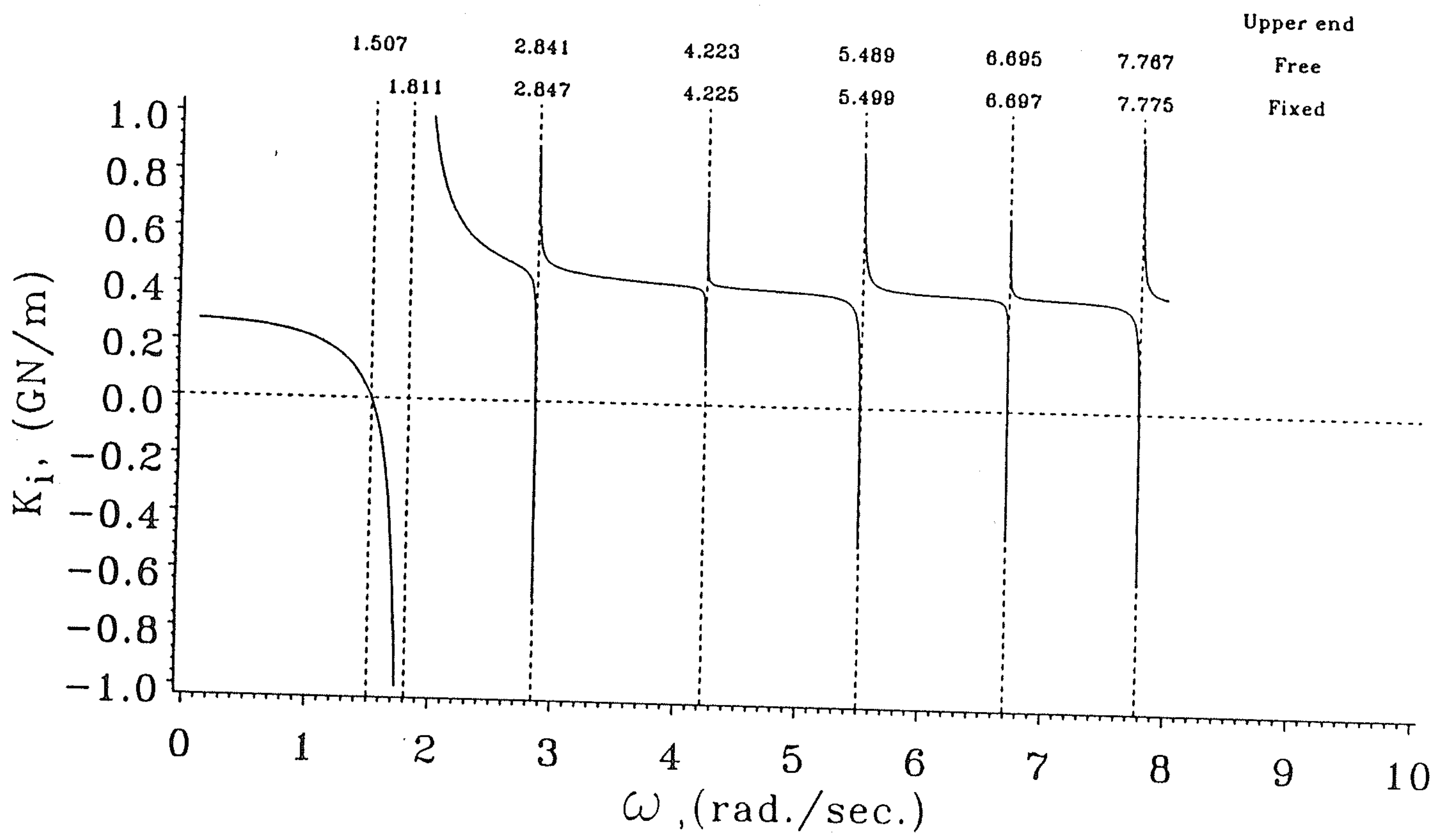

Figure 3.3(c) Variation of in-plane dynamic stiffness with frequency for an undamped inclined cable using FEM model with 12 elements. This example corresponds to the 5th level guy of the WTMJ tower.

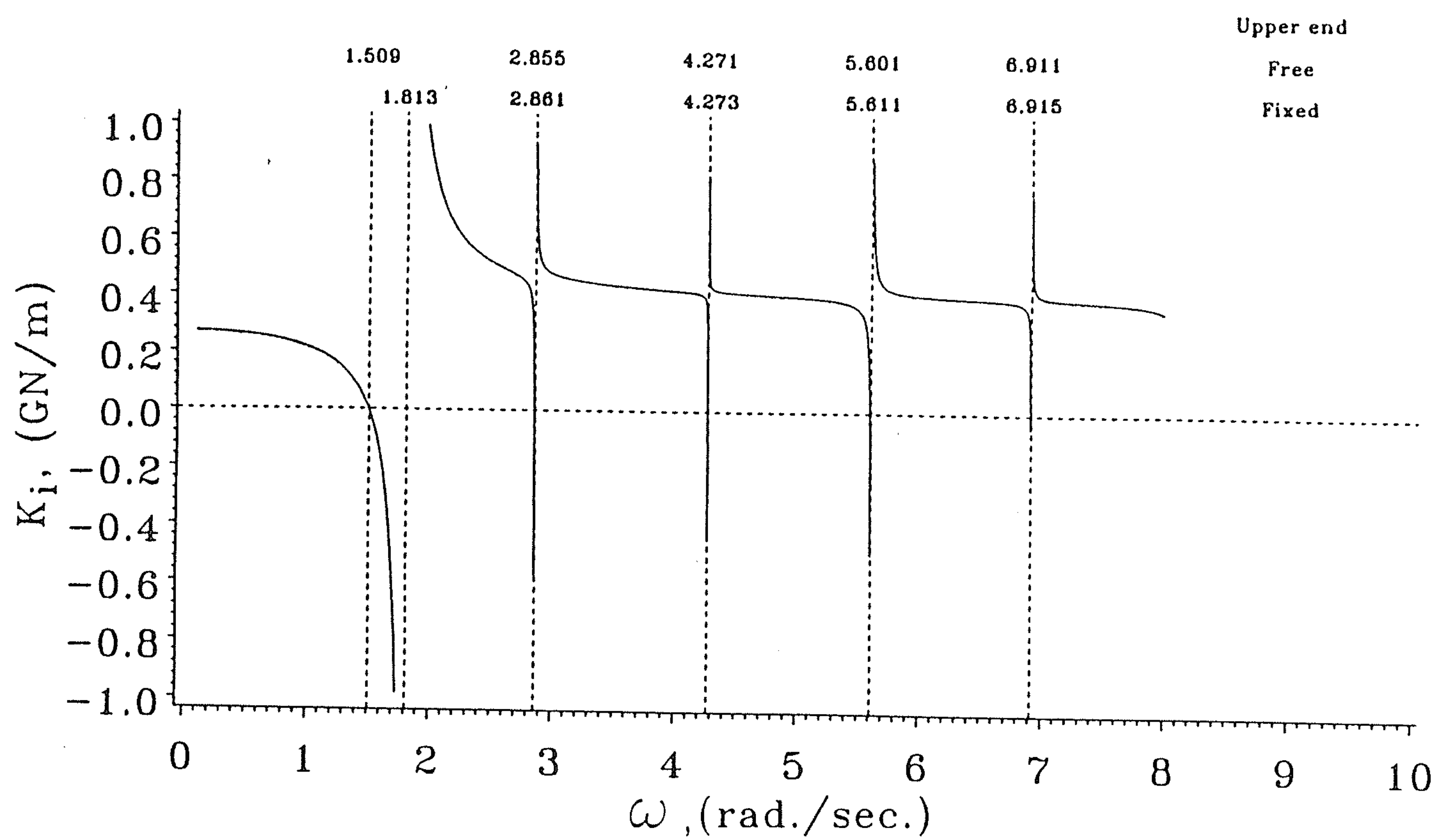

Figure 3.3(d) Variation of in-plane dynamic stiffness with frequency for an undamped inclined cable using FEM model with 16 elements. This example corresponds to the 5th level guy of the WTMJ tower.

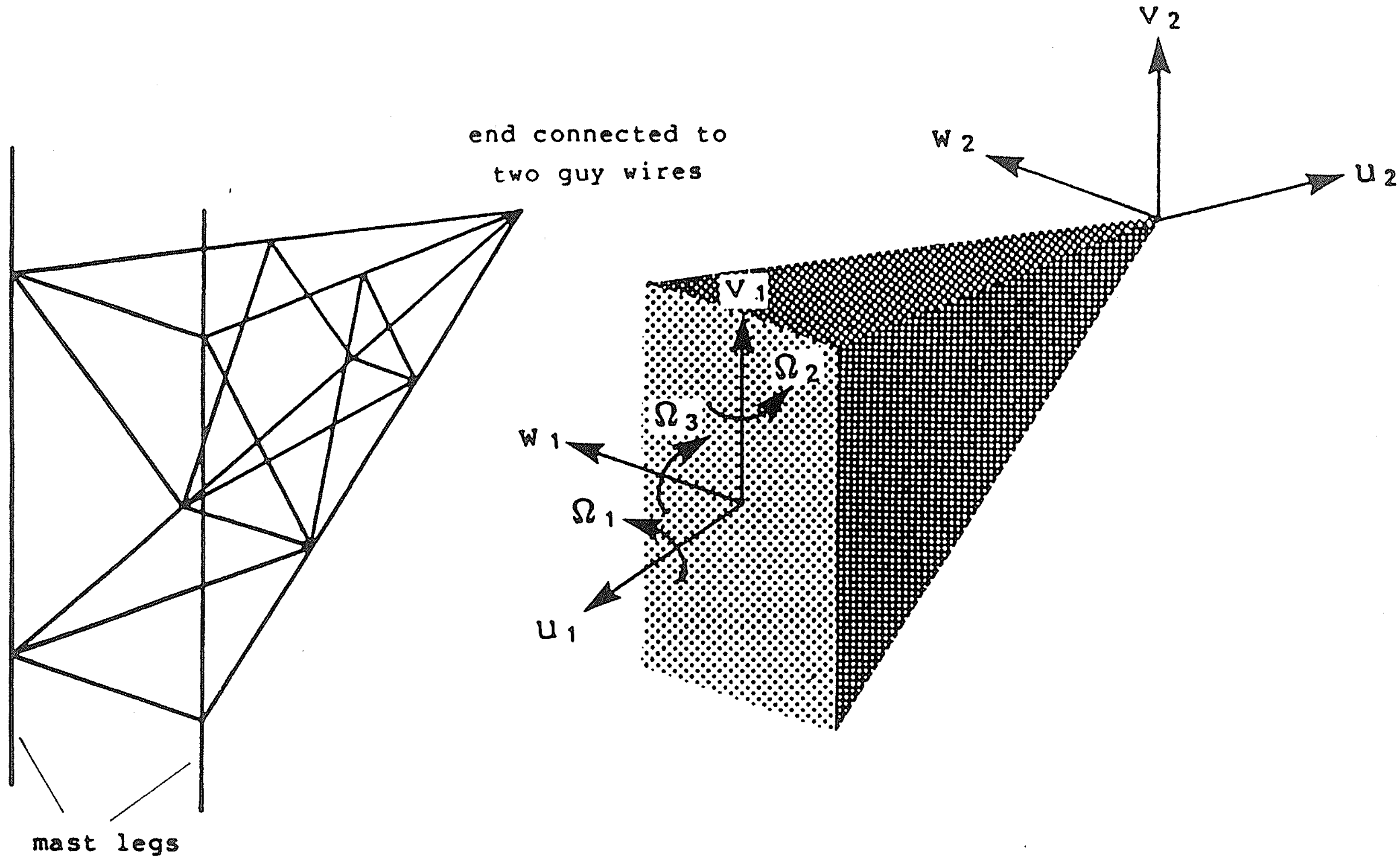

(a)

(b)

Figure 3.4 (a) A typical torque frame, and (b) its model.

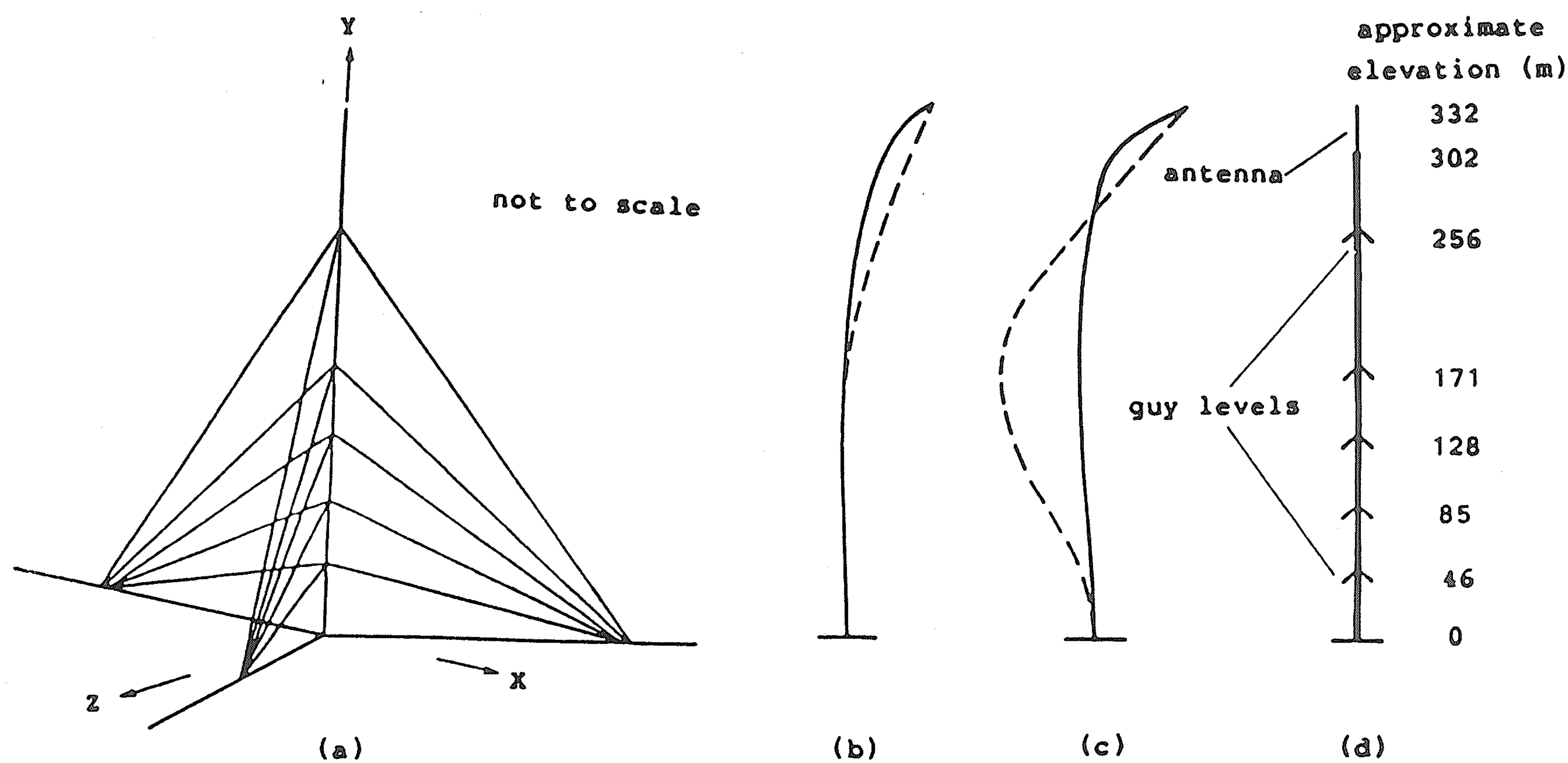

Figure 4.1 (a) The multi-level WTMJ TV tower; (b) and (c) comparison of the first and eleventh interactive normal modes, respectively (Dotted line - McCaffrey's analysis, solid line - analytical procedure and generalized finite element method.); and (d) elevations of the guy levels.

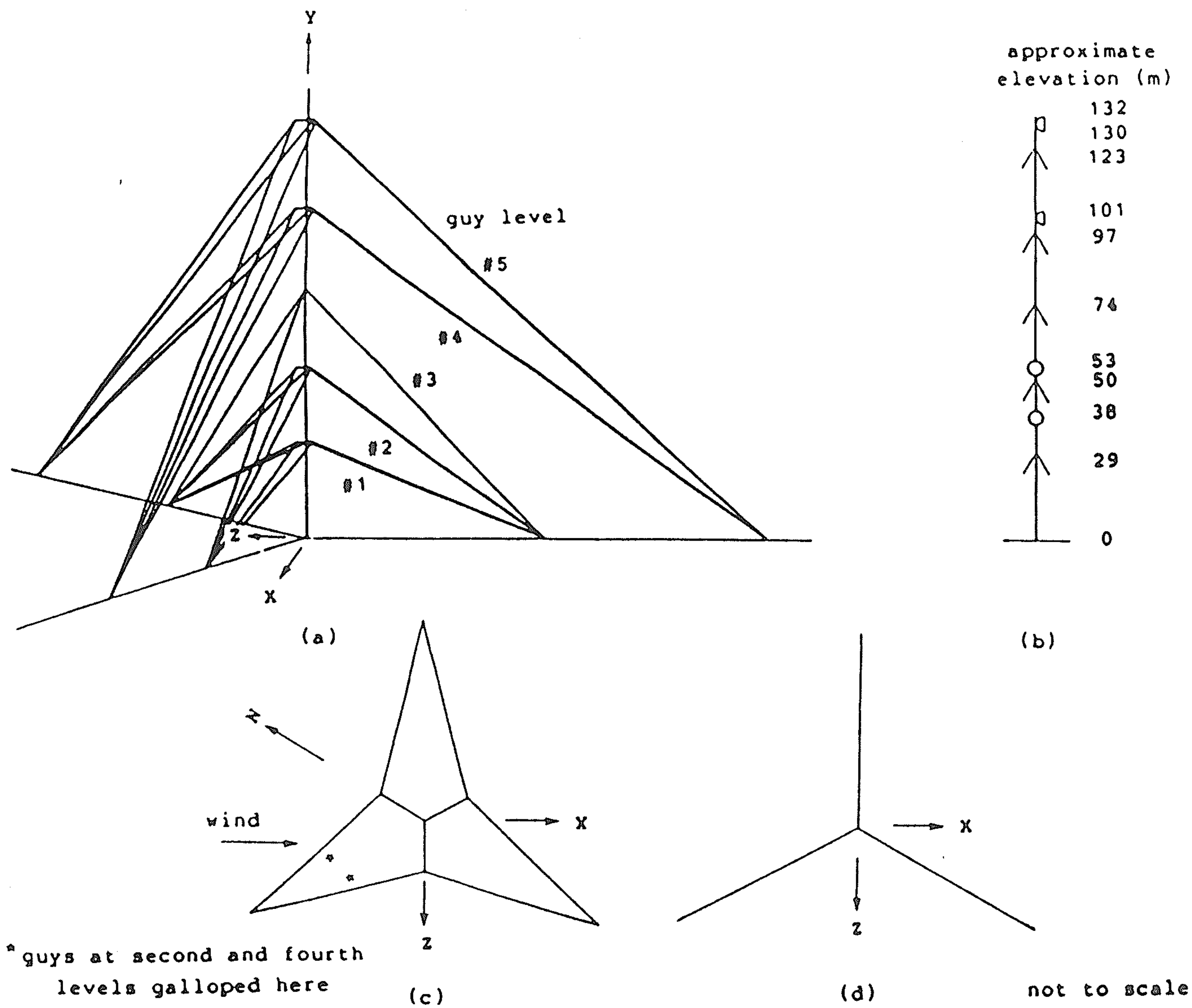

Figure 5.1 (a) The MTS guyed communication tower (antennae dishes are not shown); (b) locations of guy levels and antennae dishes; and guy arrangement at (c) 1st, 2nd, 4th and 5th levels, and (d) 3rd level.

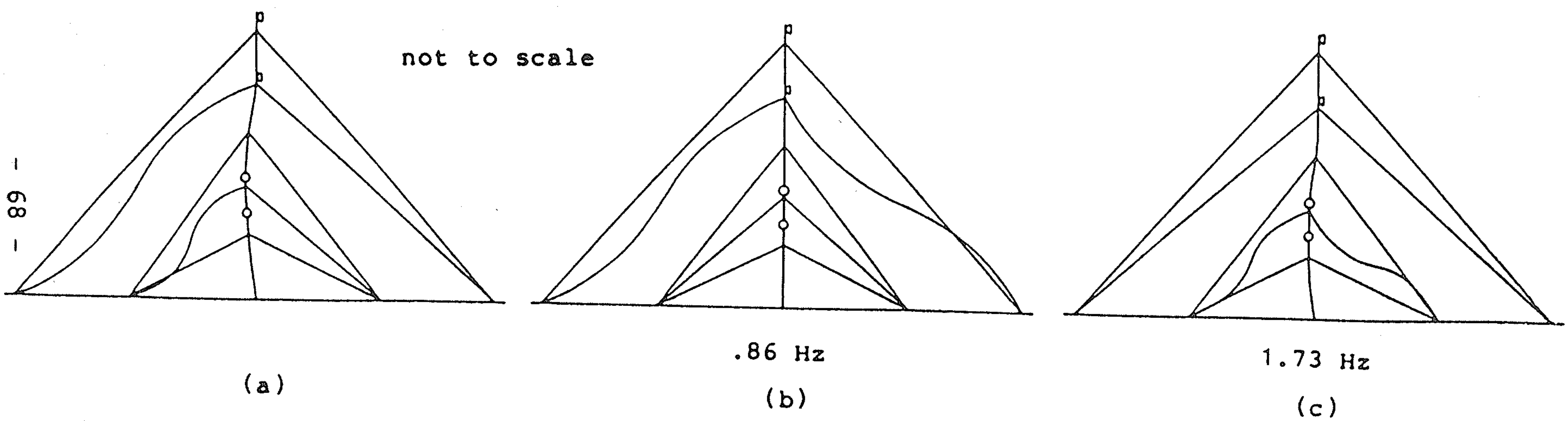

Figure 5.2 Field observations of galloping (a) which bear a close resemblance to the computed normal modes of the MTS tower, (b) and (c).

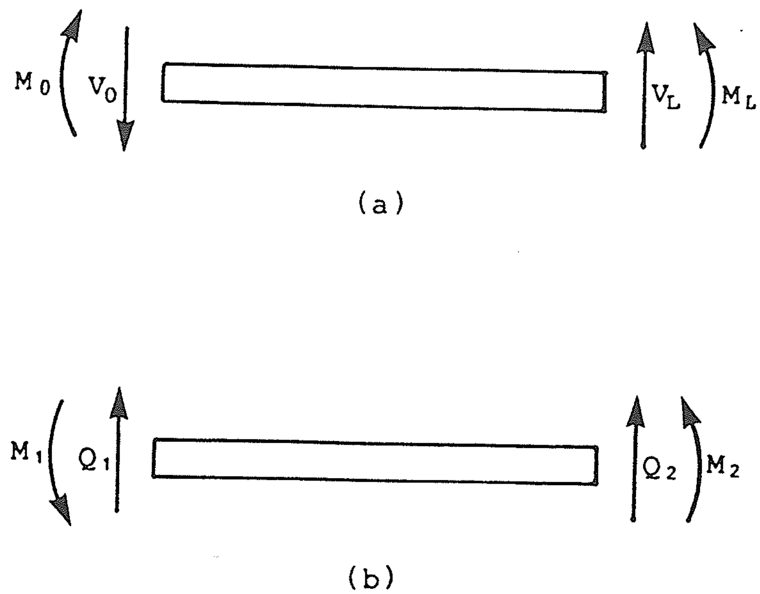

Figure A.1 Positive generalized end forces and moments
(a) "mechanics of solids" convention, and
(b) "finite element" convention.

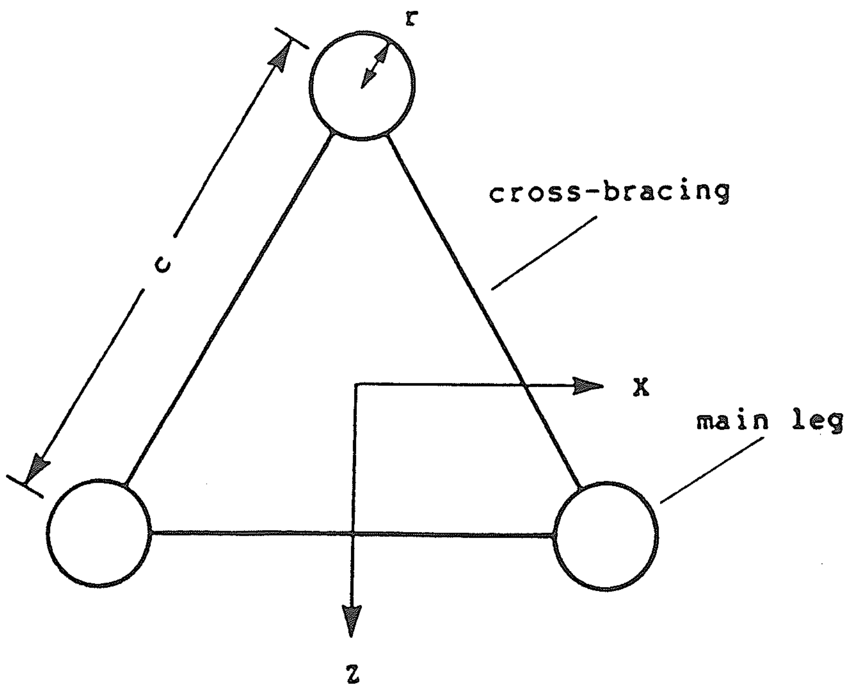

Figure B.1 Planform of the MTS tower's mast.

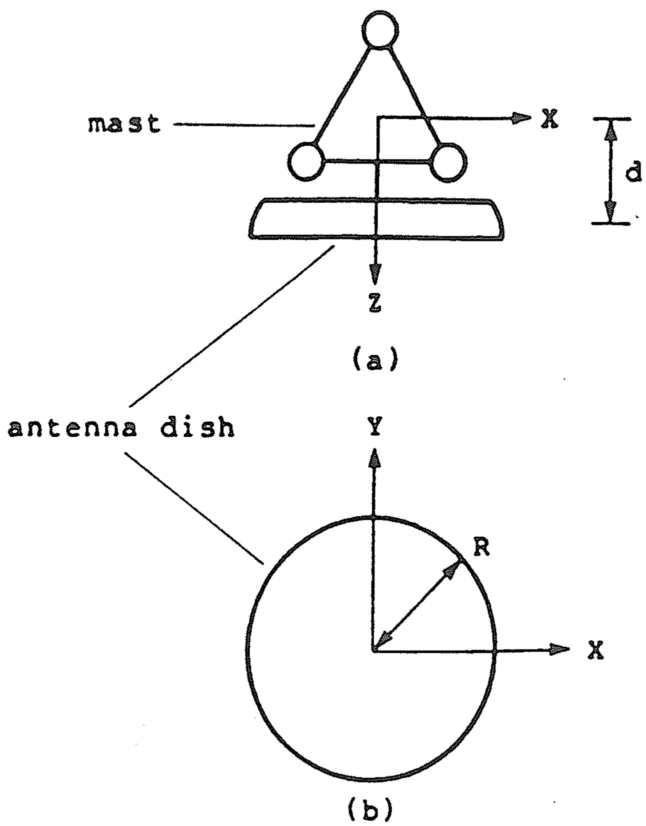

Figure B.2 (a) The planform of the mast and antenna dish of the MTS tower, and (b) the front view of an antenna dish.

	Natural frequencies, Hz.				
	Out-of-plane stiffness of guys included		Out-of-plane stiffness of guys neglected		
Mode	Analytical procedure	Generalized finite element procedure	Analytical procedure	Generalized finite element procedure	**McCaffrey's method [16]**
1^s	.2177	.2211	.2229	.2217	.2213
2	.2290	.2287			
3^s	.2338	.2346			
4	.2895	.2752			
5	.3096	.3085			
6	.3099	.3087			
7	.3226	.3224			
8	.3299	.3232			
9	.3263	.3259			
10	.3271	.3264			
11^s	.3415	.3386	.3400	.3378	.3414

Table 4.1 A comparison of the natural frequencies of the guyed WTMJ tower predicted by different procedures.(Superscript s indicates strong interactions between the mast and guys.)

Natural frequencies (in Hz.) with out-of-plane guy stiffnesses neglected		
Analytical procedure	Generalized finite element procedure	McCaffrey's method [16]
.2229	.2217	.2213
.3400	.3378	.3414
.3676	.3660	.3914
.3904	.3869	.4468
.4575	.4461	.4748
.4672	.4607	.4759

Table 4.2 Lowest six in-plane natural frequencies of the WTMJ tower.

Natural frequencies, Hz				
no axial load and ice free	axial load included but ice free			axial load and 3/8"(9.5 mm) ice
20°C	20°C	0°C	−12°C	0°C
				1.35
1.47	1.46			
				1.49
		1.52	1.53	
1.60	1.59			1.59
				1.62
		1.67		
			1.73	
				1.89
		2.38	2.38	2.38
	2.43	2.44	2.43	2.41
2.51			2.50	
				2.52
				2.56

Table 5.1 The interactive modes of the MTS tower tabulated on a linear vertical scale according to the corresponding natural frequencies.